

國立臺灣大學生命科學院生化科學所



碩士論文

Graduate Institute of Biochemical Sciences

College of Life Science

National Taiwan University

Master Thesis

廣效A/B型流感疫苗的開發

Development of a Broad-Spectrum Influenza A/B vaccine

李光正

Kuang-Cheng Lee

指導教授：翁啟惠 博士

Advisor: Chi-Huey Wong, Ph.D.

中華民國 111 年 9 月

September, 2022



致謝

回顧這兩年，時光匆匆，轉眼間就到了要畢業的時候，很感謝有這個機會來到翁啟惠老師的實驗室中學習，雖然沒跟翁老師您見到幾次面，但很感謝你總在百忙之間撥出時間指導我，並提供我實驗室那麼多的資源，從大學基礎知識的學習到這邊的實際應用是有很大的差別的，所以很感謝一開始翁老師、鄭婷仁老師、馬徹老師幫我完善我的想法使其成為一個合理的題目，更感謝鄭婷仁老師和家彥、文鳳、雅智、心瑜、世吉、俊毅、翊偉學長姐們，花了很多的時間撥空出來教我實驗技術，以及幫我釐清實驗上遇到的問題，特別是鄭婷仁老師對您的感謝無法三言兩語就寫完，也感謝質譜儀核心的學長姐幫我分析了 peptides and glycan-profile，也特別感謝辰祐學長、生醫轉譯中心協助我們包裹 mRNA，也謝謝平常在基因體中心對我的大小事提供幫助的各位，雖然只有短短兩年的時光，但沒有大家的幫助我無法獨自完成這兩年的學業。

回首了我做過的實驗，的確這兩年真的過得很充實，有了很多想法，也都一一去實行，雖然有的失敗，但也有的得到了意料之外的好結果，只期望我的實驗的確有對學界、社會的疫苗發展提供了一小步的進展，在最後的口試，很榮幸請到了翁啟惠老師、馬徹老師以及林國儀老師，雖然我們只能以線上會議的方式進行，但你們的指教我都有收到了，感謝你們撥空來參加。

最後，我人生的碩士生涯和實驗要在此告一段落了，期許下個階段自己還是能保持同樣的心態，更積極的去面對下一階段的人生，找到屬於自己的人生目標！



中文摘要

季節性流感是一種急性呼吸道症候群由數種在全世界傳播的流行性感冒病毒(Influenza virus)所引起的疾病。大部分的人得到只會有輕微的症狀和發燒並且可以康復。然而，流感病毒對某些族群會引起嚴重的症狀甚至死亡，特別是新生兒、老年人、慢性病患者及缺乏醫療資源的地區。如今，科學家尚未解決對抗未來新型流感病毒疫苗及藥物的需求。世界衛生組織每年都會預測下一年流行哪些流感病毒株，以便準時製作出下一個年度的流感疫苗。這樣設計的季節性流感疫苗可以預防特定的流感病毒株，但這樣限制了疫苗的保護效果，而且必須每年重新製造以針對即將出現的流感病毒株。因此，去研發一個可以保護多種流感病株的廣效型流感疫苗對社會大眾是非常重要的。我的研究目的就是去研發同時具有 B 型流感病毒血凝集素(Hemagglutinin)和 A 型流感病毒血凝集素組成的嵌合型血凝集素(Chimeric Hemagglutinin)疫苗作為對抗季節性流感以及尚未出現的新型流感的有效工具。在此研究中，我設計出了特別的嵌合型血凝集素蛋白並將其產出。接續研究了此重組蛋白的構型和評估它的免疫反應。結果顯示了嵌合型血凝集素蛋白可以使免疫系統產生抗體對抗四種主要的流感病毒血凝集素(H1, H3, Victoria, Yamagata)並且可以引起 CD4⁺ and CD8⁺ T 細胞免疫反應。所以，此種嵌合型血凝集素是具有潛力開發成對付流感病毒感染的廣效型疫苗。

關鍵字：流行性感冒病毒、廣效型疫苗、嵌合型血凝集素、信使 RNA 疫苗、免疫



ABSTRACT

Seasonal influenza is an acute respiratory disease caused by different types of influenza virus which are circulated in all parts of the world. Most people who get influenza can recover from fever and slight symptoms. However, influenza can cause severe illness or even death particularly in newborns, the elderly, and those with underlined disease or without medical treatments. Nowadays, combating the ongoing epidemic influenza is an unmet medical need. Every year the World Health Organization makes predictions on which influenza strains will circulate in the following year so that a vaccine can be designed, manufactured and administered to the public on time. Seasonal influenza vaccines thus designed can protect against specific viral strains but have to be renewed annually to target the upcoming strains, which limits their protective breadth and efficacy. Therefore, developing a universal influenza vaccine which is broadly protective against diverse influenza virus strains would have a great benefit to public health. My research goal is to design a chimeric hemagglutinin (cHA) that contains the head domain from influenza virus B and the stem domain from influenza A to induce broadly protective activity against seasonal influenza and unexpected pandemic influenza. cHA was designed and expressed. The properties of the recombinant protein were further characterized and used for evaluation of the immune response. Moreover, the effects of *N*-glycosylation on immunogenicity induced by HA nucleoside vaccine were also evaluated. The result showed that cHA protein can elicit significant IgG titer against variants of HA among H1, H3, Vic and Yam and CD8⁺ and CD4⁺ T cell response, suggesting that the cHA has the potential to be a universal vaccine.

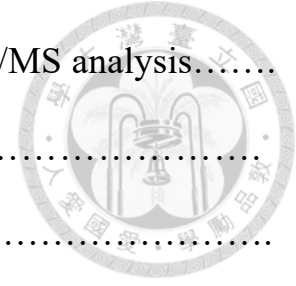
Keywords : Influenza virus, Universal vaccine, Chimeric hemagglutinin, mRNA vaccine,

Immunity

Table of contents



Acknowledgement.....	i
Chinese abstract.....	ii
English abstract.....	iii
Table of contents.....	iv
Figures.....	vii
Tables.....	ix
List of abbreviations.....	x
1. INTRODUCTION.....	1
2. MATERIALS AND METHODS.....	6
2.1 Materials.....	6
2.2 Chimeric and consensus hemagglutinin protein design.....	6
2.3 Construction of cHA protein expression plasmid.....	7
2.4 Plasmid construction for HA mRNA production.....	7
2.5 In vitro transcription.....	8
2.6 cHA protein expression and purification.....	8
2.7 Expression of mRNA in HEK293 cells.....	9
2.8 Size exclusion chromatography.....	10
2.9 Sodium dodecyl sulfate-polyacrylamide gel electrophoresis (SDS-PAGE) and Western blotting.....	10



2.10 Protein identification and Glycan profiling by LC-MS/MS analysis.....	11
2.11 Lipid nanoparticle encapsulation of the mRNA.....	12
2.12 Formulation mRNA-nanocarrier complex.....	13
2.13 Size measurement of lipid nanoparticles.....	13
2.14 Quantification of mRNA loading in lipid nanoparticles.....	13
2.15 Animal immunization.....	14
2.16 ELISA analysis.....	14
2.17 Enzyme linked immunospot (ELISpot) assay.....	15
3. RESULTS.....	17
Part I. Design of Chimeric HA as a universal vaccine.....	17
I.1 Design of a universal vaccine.....	17
I.2 In vitro expression of designed chimeric HA.....	18
I.3 Purification of cHA protein.....	18
I.4 Characterization of cHA protein.....	19
I.5 The immunogenicity of cHA vaccine.....	20
Part II. Effects of glycosylation on HA mRNA vaccine.....	22
II.1 Production of HA and HAdG mRNA.....	22
II.2 Production and characterization of HA and HAdG from mRNA-transfected cells.....	23
II.3 Characterization of HA and HAdG from mRNA-transfected cells.	23
II.4 Encapsulation of mRNA with lipid nanoparticle.....	24
II.5 Protein expression in mRNA-LNP transfected cells.....	25

II.6 Immunogenicity of mRNA-LNP.....	26
4. DISCUSSION.....	28
5. REFFERENCES.....	30

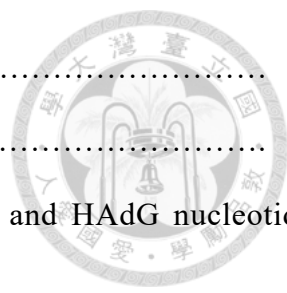


Figures



Figure 1.	The workflow of chimeric HA design.....	37
Figure 2.	The phylogenetic tree of HA subtypes that were constructed with HA sequences extracted from GISAID database by MEGA 11 software.....	38
Figure 3.	Sequence comparison of HA sequences obtained from GISAID database and used for cHA design.....	39
Figure 4.	The proteins sequences of chimeric HA.....	40
Figure 5.	The design and expression of recombinant cHA proteins.....	41
Figure 6.	The final sequence of chimeric HA used in this study. The cHA352 was aligned with conTypeA and conTypeB.....	42
Figure 7.	Purification of cHA with Ni ⁺⁺ Sepharose chromatography and DEAE Sepharose chromatography.....	43
Figure 8.	Protein identification of cHA by LC-MS/MS analysis.....	44
Figure 9.	Glycan-profiling of cHA by LC-MS/MS.....	45
Figure 10.	cHA protein characterization by size exclusion chromatography.....	47
Figure 11.	Animal experiment time-line and immunogenicity of cHA.....	48
Figure 12.	ELISpot analysis of splenocytes from cHA immunized mice.....	49
Figure 13.	mRNA synthesis constructions.....	50
Figure 14.	Agarose gel of in vitro transcript mRNA and western blotting of mRNA transfected cell.....	51
Figure 15.	LC-MS/MS of mRNA translated HA and HA _d G protein identification.....	52
Figure 16.	HA And HA _d G protein size determined by size exclusion chromatography.....	53
Figure 17.	Size distribution of prepared mRNA-Lipid nanoparticle.....	54

Figure 18. mRNA-Lipid nanoparticle encapsulation efficiency.....	55
Figure 19. Western blotting of mRNA-LNP transfected cell.....	56
Figure 20. Animal experiment time line and immunogenicity of HA and HAdG nucleotides vaccine.....	57
Figure 21. ELISpot analysis of splenocytes from HA and HAdG mRNA immunized mice...	58



Tables



Table 1. The primers used for mutation of *N*-glycosylation sites..... 59

List of abbreviations



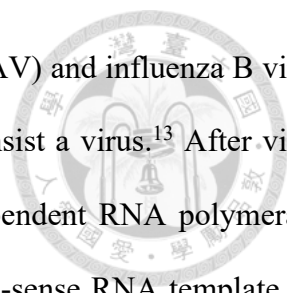
cHA	Chimeric Hemagglutinin
WHO	World Health Organization
VE	Vaccine Effectiveness
IAV	Influenza A Virus
IBV	Influenza B Virus
HA	Hemagglutinin
NA	Neuraminidase
GSAID	Global Initiative on Sharing Avian Influenza Data
TEAB	Triethylammonium bicarbonate
DSPC	1,2-distearoyl-sn-glycero-3-phosphocholine
DOTAP	1,2-dioleoyl-3-trimethylammonium-propane
DMG-PEG 2000	1,2-Dimyristoyl-rac-glycero-3-methoxypolyethylene glycol-2000
PDI	Polydispersity Index
RI	Refractive Index
HRP	Horseradish Peroxidase
PTM	Post-Translational Modification
CTM	Co-Translational Modification
SEC	Size Exclusion Chromatography
SDS-PAGE	Sodium Dodecyl Sulfate-Polyacrylamide Gel Electrophoresis
ELISA	Enzyme-Linked Immunosorbent Assay
ELISpot	Enzyme-Linked Immune Absorbent Spot
IgG	Immunoglobulin G

1. INTRODUCTION



Every year, there are 5% to 20% people infected by influenza virus.¹ The patients infected with influenza will suffer from several symptoms. The mild symptoms can be cough, fever, sore throat, headache, muscle pain and fatigue and patients will recover from flu within two weeks. However, the symptoms can be severe in newborns, the elderly, and those with underlined disease or without medical treatments. The flu often develops complications like pneumonia, leading to death.² In the modern history, there are pandemic influenza outbreak fresh in our memory: 1918 Spanish H1N1 causes more than 40 million deaths, 1957 H2N2 emerges, 1968 H3N2 begins to spread until now and 2009 H1N1 has transferred from pigs to human beings.^{3, 4} After pandemic influenza outbreaks, new type of influenza virus enters the human population and becomes a seasonal epidemic in our society.⁵ To combat the influenza virus infection, 90 years ago the first live attenuated vaccine appeared in 90 years ago. Since 1973, there are quadrivalent vaccine formulation given by the WHO every year. On the other hand, the antiviral drugs have been developed to interfere with the ability of virus spreading.⁶ According to U.S. Flu VE Network estimation, the effectiveness of influenza vaccine can be varied from 20%-60% different years.⁷ Nonetheless, the antigenic shift of influenza virus generates new ability to resist the vaccines.⁸ Therefore, to develop a more effective and precise vaccine that can provide broad protection combating the influenza virus is urgent needed.

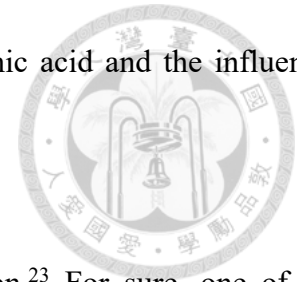
Influenza viruses belongs to the *Orthomyxoviridae* family. Most of viruses in *Orthomyxoviridae* family are capsulated by envelope containing several segmented, negative-sense, single-strand RNA segments.⁹ There are four influenza virus subtypes: A, B, C, and D. They are all zoonotic pathogen and circulating in animals, such as human, pigs, horse, birds and cattle.^{10, 11} Only influenza A and



influenza B mainly cause pandemic in human.^{11, 12} In influenza A virus (IAV) and influenza B virus (IBV), there are 8 RNA segments which encode 11 or 12 proteins to consist a virus.¹³ After virus entry, three RNA segments, PA, PB1, and PB2 encoded viral RNA-dependent RNA polymerase complex transcribes a positive-sense viral RNA template from a negative-sense RNA template. M encodes the matrix protein M1 and ion channel M2 on the virus membrane, which help virus acidification in endocytic vesicle. Nucleoprotein (NP) encodes the nucleoprotein. NS can encode non-structural protein NS1 to resist host antiviral response and nuclear export protein NS2 (NEP). Most important, HA and NA encode the surface glycoprotein hemagglutinin (HA) and neuraminidase (NA) for the important task, to control virus entry and exit the host.^{3, 5, 12-14}

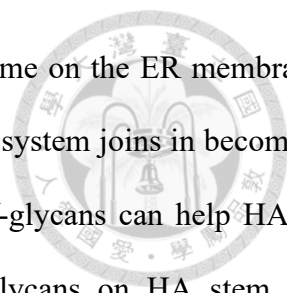
Upon the virus entry, HA will take part in recognizing their target cells. HA contains a receptor binding site to target oligosaccharides with *N*-acetylneuraminic acid (Sialic acid) capping on the cell.¹⁵ Once multiple trimetric HA recognizes and attaches to the sialic acid, neuraminidase would cleave neuraminic acid and host cell will activate endocytosis to inhale the influenza virus.^{16, 17} After entering the cell, the influenza virus is coated by the endosome. While the endosome moves close to the nucleus, the acidic environment in the late endosome will trigger trimeric HA going through conformational changes. Virus membrane then attaches and fuses to the endosome membrane by HA. Subsequently, the influenza virus membrane fuses to the endosome membrane and viral ribonucleoproteins are released into the cytoplasm and enter the host nucleus. In the nucleus, virus RNA segments replicate and are transcribed into mRNA for viral protein.^{17, 18} The mRNA is transcribed by virus RNA polymerase with host mRNA cap and as primer to begin synthesis.¹⁹ The complete translated viral ribonucleoproteins are translocated to the cytosol with M1 and nuclear export protein (NEP) helping.²⁰ All the influenza virus components including virus protein and RNA segment come close to the cell membrane for virus exit.²¹ The influenza virus uses host lipid bilayer as envelop to encapsulate its components.²¹ Upon the virus particle formation,

NA cleaves the conjugation with the host cell surface N-acetylneuraminic acid and the influenza virus can be released to attack another cell or seek out other host.²²



The influenza virus RNA amplification is an error-prone replication.²³ For sure, one of its indispensable surface protein HA also goes through lots of mutation due to its own replication mechanism. Gene mutation seems a bad thing in general but a lot of viruses, including influenza virus, use this way to avoid host immune response.²⁴ Moreover, IAV HA subtypes can be classified into two groups, group 1 and 2. H1 subtypes belong to group 1 while H3 subtypes belong to group 2.²⁵ Among the IAV two groups, their amino acid sequence identity is only 40%. Among two IBV lineages: Victoria and Yamagata, their amino acid sequence difference is up to 10%. So, the WHO annual quadrivalent vaccine formulation aims for H1, H3, Vic, Yam, four subtypes and lineage of influenza viruses mainly circulating in human.

The diverse oligosaccharides linking to the protein on Asparagine side chain amine nitrogen called *N*-glycan. This special modification takes place in Endoplasmic Reticulum and Golgi Apparatus, where has several glycan related transferase enzymes.²⁶ N-linked glycosylation occurs on a consensus sequence motif, Asn-X-Ser/Thr, where X can be any amino acids except Pro.²⁷ The process begins from the key enzyme oligosaccharyl transferase complex transfer the $\text{Glc}_3\text{Man}_9\text{GlcNAc}_2$ from dolichol-pyrophosphate to glycopeptide Asn acceptor.²⁸ Then, the *N*-glycan is further processed by several different glycosidases and glycosyltransferases and turns into three main categories of *N*-glycan: high mannose in ER and hybrid or complex in Golgi.²⁹ This kind of modification is highly common in eukaryotes and it serves as facilitating protein folding and stability, receptor binding recognition, ER transporting, membrane anchoring and proteolytic degradation protection.³⁰⁻³² As a major surface glycoprotein on the influenza virus, HA has about 6-10 *N*-linked oligosaccharides on it depending on different virus groups or its own antigenic



characteristic.^{33, 34} While the HA RNA segments turn into mRNA, ribosome on the ER membrane starts to translate HA peptide. Meanwhile, the *N*-glycosylation processing system joins in become a special modification, co-translational modification in Eukaryotes. The *N*-glycans can help HA to traverse the secreting pathway from ER to Golgi.³⁵ Besides, the *N*-glycans on HA stem are indispensable to the fusion activity and near the HA receptor binding site the glycans show cooperating with neuraminidase (NA) to release nascent virus from sialic acid.³⁶ And the glycan microheterogeneity is important to HA avoiding host immune cell recognition.³⁷ In addition, the conserved N27 glycosite among IAV HA has been reported to be important for HA folding and virus surviving.³⁸

After influenza outbreak through the world, scientists in the governments, industries and academia were dedicated to develop drugs and vaccines against influenza virus. Until now, there are several vaccines types that have been established and administered to the public such as live attenuated virus, inactivated virus and recombinant protein influenza vaccine.^{39, 40} They are designed to drive host B cell response for producing antibodies targeted the virus surface protein and neutralizing virus or elicit CD4⁺ and CD8⁺ T cell response for coordinating killer T cell eliminating target cell and antibody response to antigens from virus.⁴¹ Currently, WHO recommended seasonal influenza vaccine formulation annually, however, WHO cannot predict the circulating virus(es) exactly and the recommended vaccine may fail to provide sufficient protection against unexpected pandemic influenza virus.

In order to satisfy the desire of a single vaccine composition to prevent infection from all influenza virus, the design and development of the universal influenza vaccine has attracted a lot of attentions.⁴² Universal vaccine development on the influenza virus can be achieved by seeking out the conserved antigenic epitope on the virus surface protein and directing the immune response

toward the regions.⁴³⁻⁴⁵ To improve the protective efficacy, there are several pan-subtype chimeric hemagglutinin vaccine candidates had been reported.^{38, 46-49} Chimeric HA designs are consisting of different globular head and stem domain which are from IAV or IBV different subtypes or lineages. (i.e, combination of HAs in IAV group1 , HAs in IAV group2 or HAs in IAV and IBV) Although, they successfully elicit the host immune response but only recognize the subtype or even the group of HAs on the chimeric protein.

In this project, I try to preserve the conserved amino acids only to maximize the possibility to induce the immune response targeting the conserved region among the IAV or IBV. The conserved stem region of IAV and the conserved head region of IBV were combined to make a chimeric HA vaccine candidate (cHA), which property and immunogenicity were further characterized. Moreover, the effects of glycosylation on the immunogenicity of HA nucleotide vaccines were explored.

2. MATERIALS AND METHODS

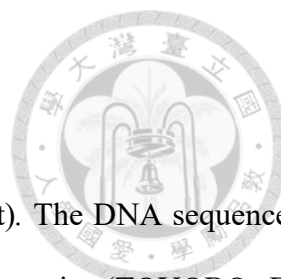


2.1 Materials

ACS chemical reagents are from Sigma-Aldrich, JT baker and Bio-Rad. The DNA polymerase KOD one is from TOYOBO. Restriction enzymes are from New England Biolabs or Thermo Scientific. DH5alpha and TOP10 competent cells are from RBC bioscience and Thermo Scientific, respectively. PCR clean up kit is from Promega. Megaprep kit is from Qiagen. The transfection reagent PEI Max and in-vivo JetRNA were purchased from Polyplus. TransIT-LT1 transfection reagent is from Mirus Bio. And Lipids used to encapsulate mRNA are from Avanti Polar Lipids. Purification Sepharoses are from GE Healthcare. And SDS-PAGE tools are from Thermo Scientific. The immunoblotting transferring buffer and apparatus are from BIO-RAD. Rapid stain for polyacrylamide gel staining is from BIOMAN. The antibodies are from PerkinElmer, Qiagen, Genetex or BEI Resources.

2.2 Chimeric and consensus hemagglutinin protein design

The hemagglutinin (HA) sequences were downloaded from 1918 to 2020 from Global Initiative on Sharing Avian Influenza Data (GSAID) database. The sequences data were sorting and alignment with Clustal Omega by python 3.7 in conda environment. The phylogenetic trees assembled by biopython with maximum likelihood method and cladogram grouping.

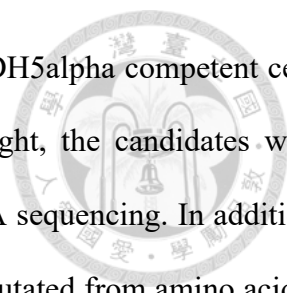


2.3 Construction of cHA protein expression plasmid

The cHA sequence was codon-optimized and synthesized (GenScript). The DNA sequence of cHA ectodomain was amplified by using KOD One™ PCR master mix (TOYOBO Bio-Technology) and specific primers containing a N-terminal secretion signal peptide from CD33 and a t4 trimerization foldon and 8xHis tag at the C-terminus. Briefly, KOD one reagent and cHA DNA were co-incubated in the automated cycler (Eppendorf) for 35 cycles of denaturation, annealing and extension. The pVax1 vector was digested with NheI and XhoI (Thermo Scientific) at 37°C for an hour with further FastAP (Thermo Scientific) for another hour. The amplified fragment and linearized pVax1 were loaded onto the well of 1% agarose gel with 6X loading dyes. Then, the cHA DNA fragment and linearized pVax1 fragment were excised from the whole gel and purified with Wizard® SV Gel and PCR Clean-Up System (Promega). Subsequently, the purified cHA fragments were cloned into pVax1 with In-Fusion® HD Cloning Kit (Clontech® Laboratories, Inc.). The reaction mixture was then used to transform the One Shot™ TOP10 Chemically Competent E. coli (Thermo Scientific) and the transformed cells were incubated at 37°C overnight. The individual colonies from the agar plate were used for direct colony PCR using Quick Taq HS DyeMix (TOYOBO Bio-Technology) to identify the colony containing desired vectors. The possible colonies were confirmed by DNA sequencing.

2.4 Plasmid construction for HA mRNA production

HA from A/California/07/2009(H1N1) were constructed in mRNA expression plasmid (pMRNA, System Biosciences) which contained T7 RNA promoter, 5'UTR, 3'UTR and C terminus poly-As. The plasmids were linearized by Eco105I and the HA sequences were amplified from a reported plasmid⁴⁹ by PCR. The fragment was gel-purified as described above and fused by using

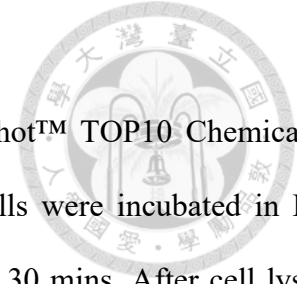


In-Fusion[®] HD Cloning Kit. After the product was transformed into the DH5alpha competent cells (RBC bioscience, Taipei, Taiwan) and the cells were incubated overnight, the candidates were selected by colony PCR and the correct plasmids were confirmed by DNA sequencing. In addition, the DNA corresponding to predicted N-glycosylation site o of HA were mutated from amino acid *N* to *Q* with site-directed mutagenesis (QuikChange Lightning Multi Site-Directed Mutagenesis Kit, Agilent Technologies) to generate HA containing no glycosylation site (HAdG). The six primers are designed to delete six N-glycosites on HA-pMRNA with DNA codon mutation from asparagine to glutamine, relatively (Table 1). After PCR amplification, the templates were digested with DpnI enzyme to remove unmutated and methylated DNA. The remaining DNA was transformed into XL10 Gold ultracompetent cells and incubated at 37°C overnight. Colonies were sent for DNA sequencing.

2.5 In vitro transcription

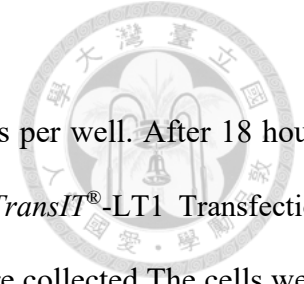
HA mRNA and HAdG mRNA were produced by using mMACHINE T7 Transcription Kit (Thermo Scientific). Briefly, the HA-pMRNA and HAdG-pMRNA were linearized with Eco105I (NEB) for an hour and the linearized DNA were incubated with T7 RNA polymerase in the presence of cap analog [m7G(5')ppp(5')G] to improve mRNA stability and translational efficiency. Subsequently, the template DNA in the mixture were removed by DNase and the mRNA was recovered by lithium chloride precipitation. Finally, mRNA concentration determined by NanoDrop. HA and HAdG mRNA were examined by loading onto a 1% agarose gel with 1X SYBR[™] Safe DNA Gel Stain (Thermo Scientific). The electrophoresis was performed with 150 volts for 15 mins. The mRNAs were then visualized with a UV transilluminator.

2.6 cHA protein expression and purification



The expression plasmids were heat-shock transformed into One Shot™ TOP10 Chemically Competent *E. coli* (Thermo Scientific) at 42°C for 30 seconds. The cells were incubated in LB buffer at 37°C overnight and collected by centrifugation at 6000 x g for 30 mins. After cell lysis, plasmids were purified by EndoFree Plasmid Mega Kit (QIAGEN) following manufacture's protocol. Sequence of plasmid DNA were confirmed by DNA sequencing. cHA-pVax1 was expressed in HEK (Human epithelial kidney) 293T cell. Before transient transfection, HEK293T cells were seeded in 15 cm dishes (Nunc) at 5×10^6 cells per dish. After incubation for eighteen hours, HEK293T cells at 80% confluency were replaced with fresh DMEM(Gibco) containing 10% FBS(Gibco) and 0.5% Antibiotic-Antimycotic (Gibco) and were transfected with expression plasmids by using PEI Max (Polysciences) using 3:1 ratio of PEI to plasmid DNA in Opti-MEM(Gibco). After 48 hrs of transfection, the medium was collected and passed through 0.2 μm vacuum filter (low protein binding, Corning). The filtered medium were then passed through Ni-NTA affinity column (GE Healthcare), the unbounded proteins were washed out with 20 mM-100 mM imidazole in buffer A (20 mM HEPES and 100 mM NaCl buffer, pH7.4). The targeted cHA proteins were eluted with 300 mM imidazole in buffer A and the eluant were further concentrated in buffer B (20mM Tris-HCl buffer, pH 7) by amicon ultrafiltration units (30K, Millipore). Subsequently, the cHA proteins in buffer B were loaded onto the Anion exchange column with (DEAE fast flow Sepharose, Cytiva). The unbounded proteins were washed out with 100 - 200 mM NaCl in buffer B. The pure cHA proteins were eluted with 500 mM NaCl in buffer B and concentrated into PBS, pH7.4. Protein concentration was determined by using the Pierce™ BCA Protein Assay Kit (Thermo Scientific). The OD₅₆₂ was measured by SpectraMax M5 Microplate Reader (Molecular Devices).

2.7 Expression of mRNA in HEK293 cells



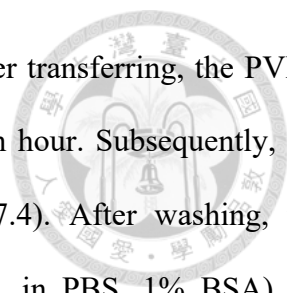
HEK 293T cells were seeded in 6-well plates (Nunc) at 3×10^5 cells per well. After 18 hours incubation, HA and HAΔG mRNA were transfected the cells by the *TransIT*[®]-LT1 Transfection Reagent (Mirus). After 18hrs of transfection, the medium and the cells were collected. The cells were treated with RIPA lysis buffer contained proteases inhibitor (EMD Millipore Corp). After 10mins incubation on ice, the mixture was centrifugated for 30mins and collected the supernatant as total cell lysate. The total cell lysate was further analyzed by size exclusion chromatography, immunoblotting and LC-MS/MS.

2.8 Size exclusion chromatography

The cHA proteins and the total cell lysate from HA-mRNA transfected cells were loaded onto the Superose[™] 6 Increase 10/300 GL or Superdex[™] 200 increase 10/300 GL (GE Healthcare) and purified in PBS with 0.75 ml/min. The standards of proteins with 43, 75, 158, 440, 660 and 2,000 kDa were loaded onto the same column for comparison. The proteins were detected by UV light. The fractions from the chromatography were further immunoblotting for analysis.

2.9 Sodium dodecyl sulfate-polyacrylamide gel electrophoresis (SDS-PAGE) and Western blotting

The cHA proteins to be analyzed were subjected to NuPAGE[™] gel (4 to 12%, Bis-Tris) and run electrophoresis in vertical gel electrophoresis device with NuPAGE[™] MOPS SDS Running Buffer (Thermo Scientific). The gels were further processed for protein staining with RAPIDstain (BIOMAN) or immunoblotting. For immunoblotting, the proteins on the gel were transferred onto the PVDF membrane using semi-dry transfer machine (Bio-Rad, Hercules) in transfer buffer (25



mM Tris, 192 mM glycine, 20% methanol (v/v), 1 % SDS, pH 8.3). After transferring, the PVDF membrane was blocked in PBS with 5% skim milk or BSA at RT for an hour. Subsequently, the membrane was washed with PBST (PBS with 0.1% Tween 20, pH7.4). After washing, the membrane was incubated with the anti-His antibody (Qiagen) (1:5000, in PBS, 1% BSA) for another hour. After washes with PBST three times at five- minute intervals, the membrane was incubated with HRP-conjugated anti-mouse IgG (PerkinElmer) (1:5000, in PBS, 1% BSA) for an hour followed by three washes with PBST. The membrane was subsequently incubated with the chemiluminescent HRP substrate (MILLIPORE) and subjected onto the trans-illuminator (FUJIFILM LAS 3000) to monitor the signals. In addition, the total cell lysates from HA-mRNA transfected cells were used immunoblotting to detect HA expression as described above. The primary Goat anti-HA antibody and the secondary anti-Goat-HRP antibody were used for immunoblotting.

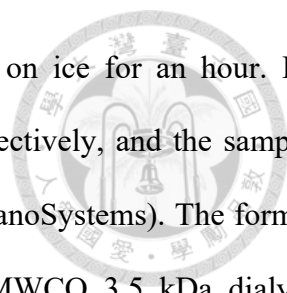
2.10 Protein identification and Glycan profiling by LC-MS/MS analysis

The interested cHA or mRNA-translated HA proteins on the gel were excised and the gel piece was stored in 50 mM Triethylammonium bicarbonate (TEAB) buffer (Thermo Scientific). The gel piece was first incubated with 50% CH₃CN (v/v) in 50 mM TEAB buffer at room temperature for 10 mins to remove the protein staining dye. After the supernatant was discarded, the gel was dehydrated with 100% CH₃CN and dried by SpeedVac evaporator (Thermo Scientific). Subsequently, the dried gel was dissolved in 10 mM TCEP and incubated at 55°C for an hour to reduce the disulfide bond. After the gel was cooled down to room temperature, 50 mM iodoacetamide was added in for alkylation and the mixture was further incubated in the dark at room temperature for 1 hour. The mixture was spinned down and the supernatant was removed followed by dehydration with 100% CH₃CN and dry by SpeedVac evaporator again. The dried gel was redissolved in the 50 mM TEAB containing trypsin (70ng/ml) and incubated at 37°C overnight. After digestion, the gel was incubated with 50% CH₃CN

containing 5% formic acid and the peptides were collected after a quick spin-down. The supernatants were further dried by SpeedVac evaporator and sent for LC-MS/MS analysis. The peptides showed up after analysis were blasted with database for protein identification. For the glycan profiling, five micrograms of interested proteins were processed through the reducing and alkylation steps as described above. Then, the proteins were digested with different combination of 0.25 μg trypsin, 0.5 μg chymotrypsin and 0.5 μg alpha-lytic protease at 37°C overnight. The peptides were dried and determined by LC-MS/MS with further glycan analysis.

2.11 Lipid nanoparticle encapsulation of the mRNA

The HA and HAdG mRNA were encapsulated with in vivo-jetRNA[®] (Polyplus) or self-assembled lipid formulation. To be encapsulated with in vivo-jetRNA[®] reagent, 1 μg mRNA were mixed with 1 μl in vivo-jetRNA[®] reagent and the mixture were diluted into desired volume with mRNA buffer and incubated at RT for 15 mins by following the manufacturer's protocol. Within an hour, the products were transfected to the cell or vaccinated the mice. Alternatively, 1,2-distearoyl-sn-glycero-3-phosphocholine (DSPC) (Sigma), cholesterol (Sigma), 1,2-dioleoyl-3-trimethylammonium-propane (DOTAP) (Sigma), and 1,2-Dimyristoyl-rac-glycero-3-methoxypolyethylene glycol-2000 (DMG-PEG 2000) (Sigma) were dissolved in the 90% ethanol and mixed in the molar ratio of 10:40:48:2 to encapsulate mRNA lipid nanoparticles using a modified syringe injection procedure or through a microfluidic mixer. For all the procedures below, mRNAs were dissolved in the 50 mM citric acid buffer (pH 4) and the final concentration of lipid is 12.5mM. The volume ratio of lipid: mRNA is set to 1: 2 and the nitrogen-to-phosphate (N/P) ratio is set to 6. The final mRNA concentration was calculated with $[n] = \frac{[L] \cdot X}{FRR \cdot \frac{N}{P}}$, where $[n]$ is the concentration of mRNA, $[L]$ is the lipid mix concentration, and X is the mole fraction of ionizable cationic lipid. For syringe injection, mRNA and lipid were loaded into syringes and injected into



microtubes. The mixture was diluted 2 times with PBS and stabilized on ice for an hour. For microfluidic mixer, mRNA and lipid were loaded into the syringes, respectively, and the samples were loaded onto cartridge which were then placed in Ignite (Precision NanoSystems). The formed mRNA-LNP were diluted 2 times with PBS and dialyzed by using MWCO 3.5 kDa dialysis membrane (Spectrumlab) overnight. The mRNA-LNP were stored at 4°C until use.

2.12 Formulation mRNA-nanocarrier complex.

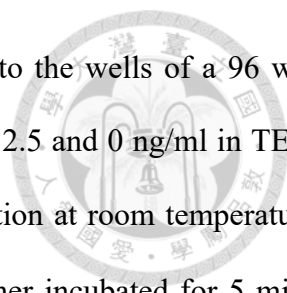
For the formulation of mRNA-nanocarrier complex, the mRNA was encapsulated in corresponding carriers using a self-assembly process. Briefly, the nanocarriers in ethanol phase (10 mg/mL) was mixed with an aqueous solution of mRNA (1 mg/mL) at pH 4.0 sodium acetate buffer in a 1 to 3 (v/v) ratio. The mRNA complexes were mixed at room temperature for 15 min, and then dialyzed against PBS buffer (pH 7.4) using Micro Float-A-Lyzer (10 kDa MWCO, spectrum lab) overnight at 4 °C and stored at -20 °C until further use.

2.13 Size measurement of lipid nanoparticles

The mRNA-LNP were diluted with nuclease free water. The particle size and polydispersity index (PDI) were measured using Zetasizer NanoZS (Malvern Panalytical Ltd.). The dispersant (water) refractive index (RI) and viscosity values were 1.330 and 0.8872 cP, respectively.

2.14 Quantification of mRNA loading in lipid nanoparticles

The loading of mRNA in lipid nanoparticles were quantified by Quant-it™ RiboGreen RNA Assay Kit (Thermo Scientific). Briefly, the mRNA-LNPs were two-fold diluted with TE buffer or



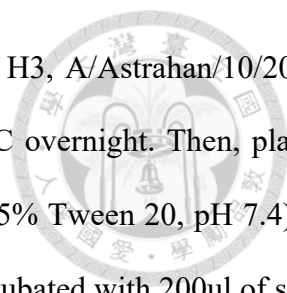
TE buffer containing 2% triton X-100. The mixture were then loaded into the wells of a 96 well plate. The 16S and 23S ribosomal mRNA were prepared as 100, 50, 25, 12.5 and 0 ng/ml in TE or 1% triton TE buffer to establish the standard curve. After 15 min incubation at room temperature, the mixture were added with 100 μ l ribogreen reagent per well and further incubated for 5 mins. The fluorescence intensity was measured by CLARIOstar® Plus (BMG Labtech) with excitation at 480 nm and emission at 520 nm. Additionally, the mRNA-LNPs in TE buffer or TE buffer containing 2% triton X-100 were subjected to agarose gel electrophoresis as described above.

2.15 Animal immunization

Female 6 to 8 weeks old Balb/c mice (three mice per group) were immunized twice intramuscularly with cHA protein or encapsulated HA mRNA at two-week intervals. Twenty micro-grams cHA proteins were formulated in endotoxin-free water and mixed with fifty μ g aluminum hydroxide (Sigma). Alternatively, 100 μ g DNA in endotoxin-free water or 5 μ g mRNA encapsulated by in-vivo JetRNA, LNP (microfluidic device) or ZG nanocarrier were used for immunization. The mice were also immunized with endotoxin-free water or with 20 μ g A/California/07/2009(H1N1) HA protein as controls. Sera were collected at day 14, 21 after the initial immunization. The collected sera were incubated at 37°C for 30 mins and centrifugated at 12,000 rpm for 10 mins to recover supernatant. The supernatant were further processed for antibody analysis by using ELISA, neutralization, and ELISpot assay.

2.16 ELISA analysis

Hemagglutinin-specific IgG levels in immune sera were monitored by ELISA. Ninety-six well ELISA plate (Greiner bio-one) was coated with 100 μ l (1 μ g/ml) variant HA protein, such as

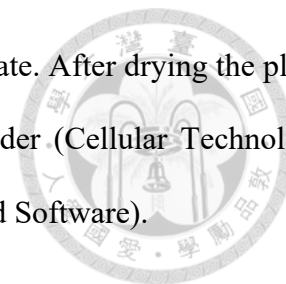


A/California/07/2009 H1, A/Brisbane/59/2007 H1, A/Wisconsin/05/2008 H3, A/Astrahan/10/2007 H3, B/Malaysia/2506/2004 Vic and B/Jilin/20/2003, and incubated at 4°C overnight. Then, plates were blocked with 1% BSA in TBST (137mM NaCl, 20mM Tris-bis, 0.05% Tween 20, pH 7.4) at 37°C for an hour and washed three times with TBST. Next, plates were incubated with 200ul of sera in two-fold serial dilutions at 37°C for an hour and washed six-times with TBST. 200ul Horseradish peroxidase (HRP)-conjugated anti-mouse antibody (1:5000) (PerkinElmer, Waltham, MA, USA) were then added into the plates incubated at 37°C for an hour, and also washed 6 times with TBST. After washed, the wells were developed with 100 µl Super Aquablue ELISA substrate (eBioscience) and the reactions were stopped by adding 100 µl 0.625 M oxalic acid. The absorbance of wells was measured at 405 nm using a SpectraMax M5 (Molecular Devices). Finally, the endpoint titer was defined as the dilution of sera absorbance two and half times higher than the optical absorbance (OD) produced by using 50-fold dilution of the sera from the mice immunized with water.

2.17 Enzyme linked immunospot (ELISpot) assay

On Day 21, mice were sacrificed and collected the splenocytes. Anti-mouse IFN- γ , IL-4 (Mabtech) or granzyme B (R&D Systems) ELISpot kits were used by following the manufacturer's instructions. The plates were washed four times and incubated for 30 min with RPMI-1640 supplemented with 10 % Fetal bovine serum (Gibco). The splenocytes were cultured at 50,000 cells per well at 37 °C in 5% CO₂ for 24 h with specific peptides from HA or HA proteins for restimulation. After incubation, the cultured medium was discarded and incubated with biotinylated anti-mouse IFN- γ , IL-4 or granzyme B specific antibody for two and half an hour. The plates were washed five times before adding the streptavidin-ALP antibody and incubated at RT for two hours.

Subsequently, the plates were wash and developed with BCIP/NPT substrate. After drying the plate, the number of resulting spots was analyzed with an Immune Spot Reader (Cellular Technology Ltd.). And Statistical analyses were done by the program Prism (GraphPad Software).



3. RESULTS

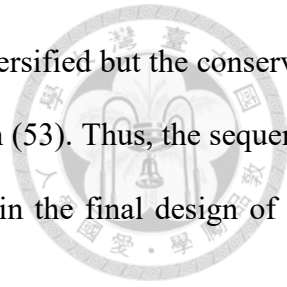


Part I Design of Chimeric HA as universal vaccine

I.1 Design of a universal vaccine

A universal vaccine was designed as shown on Figure 1. Four HA, H1 and H3 of influenza virus A as well as Victoria and Yamagata lineages of influenza virus B, were chosen as the templates for designing a universal vaccine because they respectively belong to IAV group 1, IAV group 2 and two lineages of IBV (Figure 2) and represents the main circulating strains in humans. To start the design, HA sequences of H1, H3, Victoria, and Yamagata (from 1918 to 2020) were downloaded from the Global Initiative on Sharing Avian Influenza Data (GISAID) website. The sequences that are duplicated or originated from laboratory were excluded for analysis. The remaining sequences (61,655 sequences for H1, 75,423 for H3, 17,174 for Yamagata, and 21,891 for Victoria HA, Figure 3) were aligned and used to construct the neighbor-joining phylogenetic tree to group the sequences into various clades/subtypes. The consensus sequence was first created for each clade. Subsequently, these consensus sequences in every clade were aligned again to deduce the consensus sequence. Unfortunately, this attempt was failed. Therefore, I decided to divide the consensus clade sequences into two groups: group A consists of the consensus clade sequence from H1 and from H3; group B consists of the consensus clade sequence from Victoria and from Yamagata. Although the full-length H1 shows low identity (40%) to H3, the sequence identities in HA1 and HA2 are 31% and 65%, respectively (Figure 3). On the other hand, HAs in group B show high identity (98%). As a result, a chimeric HA was designed (Figure 4A) to have the HA1 domain of the consensus sequence deduced from the sequences in group B (conTypeB, Figure 4B) and the HA2 domain of the consensus sequence from the sequences in group A (conTypeA,

Figure 4C). Furthermore, the stem region on conTypeA HA2 is highly diversified but the conserved cysteine linker needs to be preserved for linking the head and stem domain (53). Thus, the sequence of GKLC from the stem region on HA1 from conTypeA was preserved in the final design of the chimeric HA (cHA) (Figure 4A).

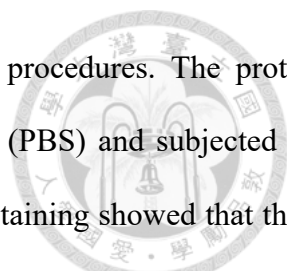


I.2 In vitro expression of designed chimeric HA

For expression and purification of cHA recombinant proteins from HEK293 cells, the cHA was designed to have an N-terminal CD33 signal peptide to promote secretion, a C-terminal T4 trimerization foldon to enhance cHA folding and a tag of eight histidines to facilitate the purification and the detection (Figure 5A). The gene fragments encoding different domains of cHA was amplified from various HA consensus sequences by PCR and the amplified fragment were subsequently assembled into pVax1 vector to construct a cHA expression vector. The HEK293T cells were then transfected with cHA expression vector. After 48 hours incubation, the medium were collected and processed for immunoblotting analysis. The initial attempt to express the full-length cHA (cHA498) failed (Figure 5B). The expression vector for genes encoding C-terminally truncated cHA (cHA462 and cHA352) were thus prepared and used for expression tests. As shown in Figure 5B, cHA352 can be successfully expressed in HEK293 cells and is used for the subsequent works. Compared to the sequences of conTypeA and conTypeB, it was notices that majority of HA2 were deleted to confer expression for cHA-352 (Figure 6).

I.3 Purification of cHA protein

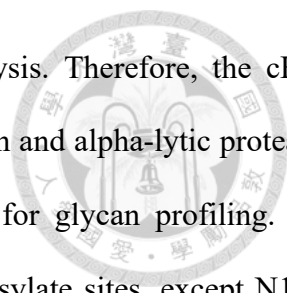
For purification of cHA proteins, the medium of the cells expressing cHA were collected and



purified with the Ni⁺⁺ Sepharose column by using the manufacturer's procedures. The protein fractions from each step were concentrated in phosphate buffered saline (PBS) and subjected for SDS-PAGE and western blotting analysis (Figure 7A). Although protein staining showed that there are multiple proteins bands in the fractions eluted with 300 mM imidazole (SDS-PAGE in Figure 7A), the immunoblotting analysis indicated that a region with apparent molecular weight of 70 kDa in the fractions eluted with 100 mM and 300 mM imidazole can be detected by specific antibodies recognizing penta-his tags (Figure 7A). To further purify the major proteins of apparent weight of ~70 kDa, the fractions eluted by 300 mM imidazole were further purified using anion-exchange chromatography. The protein solution was loaded on a column packed with DEAE Sepharose and the bound proteins were eluted with 0 – 500 mM NaCl in 50 mM Tris, pH 7.0. As shown in Figure 7B, a major band of apparent weight of 70 kDa can be purified. Nonetheless, a minor band around 40 – 55 kDa can be also observed in immunoblotting analysis (Figure 7A and B). To confirm the identity of purified proteins, the bands around 70 kDa and 40–55 kDa were excised for protein identification using LC-MS/MS analysis. The results confirmed that several peptides in cHA can be detected in the band around 70kDa, but not in the band with apparent molecular weight of 40~55 kDa band (Figure 8). Altogether, the cHA can be purified by using two-step purification with a yield of 11 µg per liter of HEK293 cells.

I.4 Characterization of cHA protein

The cHA proteins produced from HEK293T cells are around 70 kDa on the SDS-PAGE and the predicted cHA protein size is 45.2 kDa. Thus, it is possible that the cHA protein has post-translational modification (PTM) or co-translational modification (CTM). One of the PTM/CTM is likely to be *N*-linked glycosylation because there are 7 *N*-linked glycosylation sites predicted by NetNGlyc website (Figure 5A). In addition, the heterogeneity caused by *N*-linked glycosylation

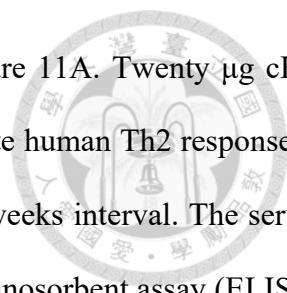


might lead to the wide appearance of the protein on SDS-PAGE analysis. Therefore, the cHA proteins were digested with different combination of trypsin, chymotrypsin and alpha-lytic protease and the peptides were subsequently subjected to LC-MS/MS analysis for glycan profiling. As shown in Figure 9, *N*-glycans can be detected on the predicted *N*- glycosylate sites, except N142 and N269. Despite several attempts of using various combinations of three proteases, no glycopeptides containing N142 or N269 can be detected using LC-MS/MS analysis. Whether there is glycan(s) on N142 or N269 cannot be determined. On the other 5 glycosites, *N*-glycans are highly diversified and most of glycans are complex-type *N*-glycan. High-mannose type *N*-glycan can be only found on N172 (Figure 9C). And N280 on cHA is conserved *N*-glycosylation site (NTSL or NSSL) in influenza A HA stem region (59) (Figure 9E)

Influenza HAs form trimers on the surface of virus and can be recombinantly expressed in a trimeric form.⁵⁰ I therefore wonder whether recombinant cHA proteins can form trimeric structure. In order to answer this question, the purified cHA proteins were loaded onto the size exclusion chromatography (SEC) to estimate the size of the molecule in the native state (Figure 10A). The proteins were passed through SEC and the fractions were collected every 1 minute. The fractions corresponding 8 ml to 20 ml elution volume were analyzed by immunoblotting. In conclusion, cHA proteins were detected on 9 ml to 13 ml elution volume, suggesting that the size of cHA secreted by HEK293T cells are between 669 kDa to 2,000 kDa (Figure 10B). The results implied that cHA proteins are possibly misfolded and aggregated. It is reasonable since cHA is a truncated protein that contains only the conserved region of HA in different groups.

I.5 The immunogenicity of cHA vaccine

After cHA protein property was confirmed, the immunogenicity was assessed by animal



experiment. The cHA protein is addressed to the mice as shown as Figure 11A. Twenty μg cHA protein were prepared with 50 μg aluminum hydroxide, which can stimulate human Th2 response to promote antibody production⁵¹, the mice were given two doses at a two-weeks interval. The serum was collected at Day 14 and Day 21 and subjected to enzyme-linked immunosorbent assay (ELISA) and enzyme-linked immune absorbent spot (ELISpot) assay. The ELISA assay used different HA protein among four subtypes, H1, H3, Vic and Yam to evaluating the protection efficacy of cHA against variant of influenza virus. Interestingly, with one dose of cHA protein the mice produced antibodies not only against cHA protein itself but also all four subtypes HA used as antigen (Figure 11B.). On Day14, the immunoglobulin G (IgG) titer showed same amount against H1 and Yam and a little bit lower against Vic. The IgG titer against H3 protein was still detectable even titer was lower than others. On Day 21, all the IgG titer against five HA proteins were significantly higher than the titer on Day 14 (Figure 11C.). The IgG titer against H1 and Yam reached 100,000 - 200,000 but the igG titer against H3 was 1600. Although the cHA proteins might form aggregation form and is truncated, the induced IgG titer implied that combination of conserved region into chimeric protein might provide an alternative design for universal vaccine. Moreover, the cHA with a short length HA2 region from conTypeA was able to produce IgG against H1 and H3 HA, suggesting that the consensus region between IAV HA could be founded on HA2. The cHA HA1 region was conserved enough for eliciting the IgG against IBV Vic and Yam HA. On the other hand, the mice were sacrificed on Day 21 and splenocytes were collected and subjected to ELISpot analysis (Figure 12.). Interferon-gamma ($\text{IFN}\gamma$), interleukin-4 (IL4) and granzymeB (GrzB) spots were detected in the wells of cHA immunized mice. The result showed that cHA protein can induce CD4^+ and CD8^+ T cell response.

The results that truncated cHA with aggregation form induced antibodies targeting H1, H3, Vic and Yam are intriguing. In the future, the cHA tertiary structure still needs to be elucidated.

Moreover, the urea refolding method may be used to help cHA refolding into correct HA tertiary trimeric conformation. Besides, the cHA with only conserved region between IAV and IBV HA can be used on mRNA vaccine platform, which conquers the chimeric protein structure integrity and manufacture time consuming.⁵² And the cHA mRNA vaccine with complete length of conserved region can be expected to be a real universal influenza vaccine.

Part II Effects of glycosylation on HA mRNA vaccine

Hemagglutinin is a protein with *N*-glycans shielded outside and the *N*-glycans might change the profiles of the exposed epitopes. It was reported that the monoglycosylated HA protein or LAIV induces higher antibody titers, more neutralization antibodies that can block influenza virus infection, and greater T and B cell immune response.^{53, 54} It was also reported that unglycosylated HA protein vaccines induce weaker immune response than monoglycosylated HA protein vaccine. In these reports, unglycosylated or monoglycosylated proteins were produced by endoglycosidase treatment of the purified glycosylated protein. I therefore wonder if HA contains no glycosylate sites can be used directly as vaccine to induce significant immune response. However, HA containing no glycosites cannot be successfully expressed and purified by using recombinant protein approach. Recently, it was found that, using the new emerged mRNA technology, a mRNA vaccine encoding the SARS-COV2 spike with glycosite-deletion can induce broader protection than a mRNA vaccine encoding with-type SARS CoV-2 spike.⁵⁵ I therefore would like to apply mRNA vaccine approach to explore whether a mRNA vaccine encoding HA with no glycosylation sites can induced significant immune response.

II.1 Production of HA and HAdG mRNA

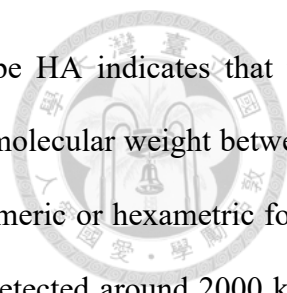
Hemagglutinin of A/California/07/2009 (H1N1) (pdm09) recommended by the The US Food and Drug Administration for use in vaccines during the 2009-2010 and 2010-2011 influenza seasons was chosen for the experiments. The genes for wild-type HA were cloned into pMRNA and the glycosylation sites were mutated by site-directed mutagenesis to give HA with no glycosites (HAdG) (Figure 13).

II.2 Production and characterization of HA and HAdG from mRNA-transfected cells

The plasmids were used for in vitro transcription and the obtained mRNA were processed for agarose gel electrophoresis to confirm the quality of mRNA (Figure 14A). Subsequently, HEK293T cells were transfected with the mRNAs and the successful expression of proteins from mRNA were monitored with western blotting. As shown in Figure 14B, wild-type HA can be expressed in the cells and detected with an apparent molecular weight of ~100 kDa. On the other hand, HAdG were expressed with an apparent molecular weight of ~70 kDa. Compared to wild-type HA, the decreased size of expressed HAdG is possibly due to loss of glycans. The corresponding protein bands were also excised and the identities of protein were further confirmed by using LC-MS/MS analysis. As shown in Figure 15, several peptides (marked in red) can be found in LC-MS/MS analysis, confirming that the protein band around 100kDa and around 70kDa represents wild-type HA and HAdG, respectively (Figure 14B).

II.3 Characterization of HA and HAdG from mRNA-transfected cells

To confirm whether HAdG can form trimers in the cells, HEK293 cells were transfected with the mRNA encoding wild-type HA or HAdG. The cells were collected and the cell lysates were subsequently fractionated by the size exclusion chromatography (Figure 16.). The immunoblot

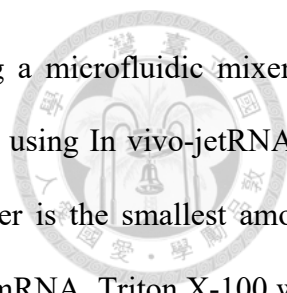


analysis of the eluted fraction for the column loaded with the wild-type HA indicates that the transfection of wild-type HA mRNA indeed produced HA proteins has a molecular weight between 158 kDa to 669 kDa and the produced HAs possibly are in the natural trimeric or hexameric form (Figure 16A and B). On the other hand, HAdG proteins were primarily detected around 2000 kDa and with lower expression amount than wild-type HA (Figure 16C and D). It is possible that HAdG forms aggregates, instead of normal trimeric conformation for wild-type HA, as the deletion of N28 can greatly influence the structural stability of HA (51, 52).

II.4 Encapsulation of mRNA with lipid nanoparticle

After confirming the expression of HA and HAdG from mRNA-transfected cell, I further prepared mRNA-lipid nanoparticle (mRNA-LNPs) to enable efficient delivery of mRNA into the cells. The mRNA in vivo delivery needs to protect mRNA from degradation. Also, delivery system needs to allow cell uptake and release mRNA into the cytoplasm. Thus, lipid nanoparticle encapsulation was subjected onto delivery of mRNA.⁵⁶ I prepared mRNA-lipid nanoparticle in four different ways. The first method is to simply use a commercial reagent In vivo-jetRNA by manufacturer's protocol. The other methods use a reported lipid mixtures composed of 1,2-distearoyl-sn-glycero-3-phosphocholine (DSPC), cholesterol, 1,2-dioleoyl-3-trimethylammonium-propane (DOTAP), and 1,2-Dimyristoyl-rac-glycero-3-methoxypolyethylene glycol-2000 (DMG-PEG2000) and the formation of lipid nanoparticles were achieved by manual syringe injection or microfluidic mixer.^{55, 57} Moreover, an arginine-rich peptides synthesized in-house (unpublished) were used as one method to deliver mRNA.

The size of formed mRNA-LNP were determined with dynamic light scattering. The polydispersity index (PDI) of mRNA-LNP formed using In vivo-jetRNA and conventional syringe



injection are around 0.25 while the PDI of mRNA-LNP prepared using a microfluidic mixer is around 0.144 (Figure 17). The results indicated that mRNA-LNP formed using In vivo-jetRNA is large and diverse while mRNA-LNP prepared using a microfluidic mixer is the smallest among these three methods (Figure 17). To quantify the amount of encapsulated mRNA, Triton X-100 was included in the solution to break lipid nanoparticles and to release the encapsulated RNA for quantification by using ribogreen. The amount of encapsulated RNA was then compared to the amount of mRNA loaded for encapsulation to calculate encapsulation efficiency. The mRNA encapsulation efficiency using In vivo-JetRNA was around 60% with high variation. On the other hand, mRNA can be almost completely encapsulated in lipid nanoparticles through manual syringe injection or microfluidic mixer (Figure 18A). Moreover, the quality of the encapsulated mRNA was monitored using agarose gel electrophoresis. As shown in Figure 18B, the mRNA-LNP with or without tritonX-100 are loaded onto the agarose gel. The bands show that mRNA-LNP cannot be run down the gel and therefore stays on the top of well due to its neutral polarity. With the addition of triton-100 to release mRNA from mRNA-LNP, released mRNA can be seen on the gel with correct size, indicating that encapsulated mRNA remains intact during the process (Figure 18B).

II.5 Protein expression in mRNA-LNP transfected cells

Whether mRNA-LNP can confer protein expression in the targeted cells was then evaluated. HEK293T cells were transfected with the formed mRNA-LNP and total cell lysate were collected 18 hrs after transfection. The collected cell lysates were subjected to immunoblotting analysis to monitor the expression of HA. HA protein and HA₂G protein on 100kDa and 70kDa, respectively, can be detected in the cells transfected with mRNA-In vivo jetRNA and with mRNA-LNP that were formed by a microfluidic device, but barely detected in the cells with mRNA-LNP formed by conventional syringe injection (Figure 19). Perhaps mRNA-LNP formed by conventional syringe

injection are less stable and therefore confers much lower expression in transfected cells.



II.6 Immunogenicity of mRNA-LNP

To evaluate the immunogenicity difference of HA and HAdG nucleoside vaccine, the mRNA-*in vivo* jetRNA were first immunized the mice. Unfortunately, the ELISA analysis showed no detectable endpoint titer against A/Cal/07/2009 H1 protein (data not shown). Thus, the mRNA-LNP and mRNA-ZG nanocarrier were further prepared and used to immunize the mice with two doses at a two-week interval. In addition, DNA plasmids encoding HA and HAdG were prepared and tested parallelly. The mice were immunized with 5 μ g mRNA-LNP, 5 μ g mRNA-ZG nanocarrier or 100 μ g DNA (Figure 20A). The serum was collected from mice on Day 14 and Day 21 for evaluating serum IgG titer against HA by ELISA analysis. After the first dose, mRNA-LNP and mRNA-ZG nanocarrier were shown to induce similar endpoint titer against wild-type HA (A/Cal/07/2009) (Figure 20B). The wild-type HA mRNA induced higher IgG titer against wild-type HA protein. However, the mRNA with all *N*-glycosites deleted induced slightly lower IgG titer against full-glycosylated wild-type HA protein, suggesting that the structure integrity or the lower expression of HAdG mRNA might affect the antibody production on mRNA vaccine. The HAdG mRNA induced a little bit higher IgG titer against H1 variants A/Bris/59/2007 than HA mRNA did (Figure 20D). Moreover, the HAdG DNA showed no detectable endpoint tier but the HA DNA elicited high IgG titer (Figure 20B and D). The results implied that DNA and mRNA vaccine might use different mechanisms to induce the antibodies, or DNA is more stable than mRNA. The mRNA vaccine showed its advantage on delivery of glycosites modified nucleoside vaccine. On Day 21, the IgG titer showed a little bit higher but no significant differences compared to the titer of the serum on Day 14 (Figure 20C and D.). Compared to other reports on mRNA vaccine, my mRNA vaccine induced lower IgG titers. It is possible that the dose in my experiments was lower than the amount

(50 µg) used in other studies. In addition, pseudouridine modified mRNA might be critical for inducing immunogenicity.^{55, 58} On the other hand, the mice splenocytes were collected and subjected to ELISpot analysis for evaluating T cell response. As shown in Figure 21, splenocytes were stimulated with different HA proteins and the amount of IFN γ - and IL-4 secreting T cells were similar in the mice immunized with, the HA and HAdG mRNA. Although the IgG titers were low after two immunizations, the IFN γ and IL4 T cell responses are significant. Since the experiments were conducted 7 days after the second immunization, the results implied that mRNA vaccine induced T cell response in the early stage and antibodies production might be in the later stage.^{59, 60}

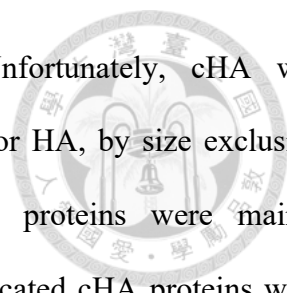


4. DISCUSSION

Every year, people in the world face not only one single influenza virus strains but different subtypes of influenza viruses that can rapidly go through gene mutations to have antigenic shift. Instead of an annually formulated vaccine, a universal vaccine that can provide unmet protectivity against variants of influenza viruses or different subtypes of influenza viruses is the light at the end of the tunnel in this field.

Hemagglutinin proteins are the major target on the influenza virus surface. Several methods for universal vaccine development have been suggested, such as unmasking hemagglutinin from its glycan shield, creating chimeric hemagglutinins by combining various domains or conserved regions from HA in specific subtypes.^{45, 47, 53} In this research project, a chimeric HA were designed by combining domains from the consensus sequences derived from H1 and H3 in influenza virus A and from HA in influenza B virus. The proteins and its immunogenicity were further characterized and assessed. On the other hand, unmasking the glycan shield of HA was evaluated using mRNA approach, that is, the glycosites of HA have been deleted by site-directed mutagenesis and the produced mRNA were used for immunogenicity evaluation.

The designed cHA is the combination of the globular head domain from the conserved Type B and a short HA1 stem as well as a conserved HA2 stem region from the consensus Type A. The head and stem domain were designed to connect with conserved Cysteine linker and its relative site on the consensus Type B. The conserved cleavage site to cleave HA0 to HA1/HA2 was also preserved in cHA. For expression and secretion into cultured medium to facilitate the purification, a signal peptide from CD33 was used. The cHA protein was successfully purified to a purity >80%



by using Nickel affinity and anion exchange chromatography. Unfortunately, cHA was characterized to be in an aggregation form, instead of a trimeric form for HA, by size exclusion chromatography. The *N*-glycan profiling results showed that cHA proteins were mainly glycosylated with complex-type *N*-glycans with great diversity. The truncated cHA proteins were found to induce the antibodies against variant subtypes of influenza HA including, H1, H3, Vic and Yam. However, lower titer against H3 protein was observed. Furthermore, cHA proteins can elicit T cell response. Taken together, the results showed that cHA has the potential to be developed as a universal influenza vaccine. In the future, the cHA delivered as mRNA vaccine can be explored and expected to have better immune response.

On the other project to evaluated the effects of HA immunogenicity by mRNA vaccine, the HA and HAdG mRNA have been successfully prepared and used to transfect HEK293 cells for in vitro protein expression. Without the critical N28 on HAdG, the HAdG was expressed as misfolded protein in aggregation form as confirmed by the size exclusion chromatography. To develop the nucleotide vaccine, several delivery methods were tested and mRNA-LNP formulated by using a microfluidic device showed the most uniform and stabilized encapsulated by the lowest PDI and encapsulation efficiency as shown in Figure 17 and 18. In addition, the immunogenicity studies of HA and HAdG showed that mRNA vaccine is advantages on conquering the protein structure integrity issue. Interestingly, mRNA, but not DNA, encodes HA with glycosites deletion can be used to induce the antibodies. However, the detailed mechanism of mRNA-induced immune response needs to be further elucidated.

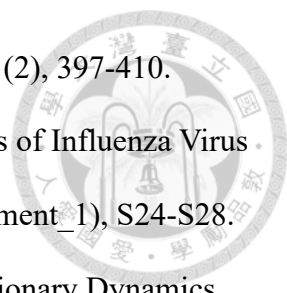
5. REFERENCE

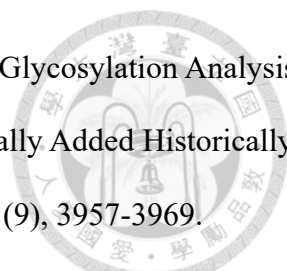


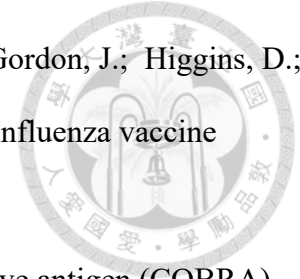
1. U.S. Centers for Disease Control and Prevention Key Facts About Influenza (Flu).
<https://www.cdc.gov/flu/about/keyfacts.htm>. (accessed August 26, 2021).
2. U.S. Centers for Disease Control and Prevention Flu Symptoms & Complications.
<https://www.cdc.gov/flu/symptoms/symptoms.htm>. (accessed September 21, 2021).
3. Krammer, F.; Smith, G. J. D.; Fouchier, R. A. M.; Peiris, M.; Kedzierska, K.; Doherty, P. C.; Palese, P.; Shaw, M. L.; Treanor, J.; Webster, R. G.; García-Sastre, A., Influenza. *Nature Reviews Disease Primers* **2018**, *4* (1), 3.
4. Short, K. R.; Kedzierska, K.; van de Sandt, C. E., Back to the Future: Lessons Learned From the 1918 Influenza Pandemic. *Frontiers in Cellular and Infection Microbiology* **2018**, *8*.
5. Petrova, V. N.; Russell, C. A., The evolution of seasonal influenza viruses. *Nat Rev Microbiol* **2018**, *16* (1), 47-60.
6. Hannoun, C., The evolving history of influenza viruses and influenza vaccines. *Expert Rev Vaccines* **2013**, *12* (9), 1085-94.
7. U.S. Centers for Disease Control and Prevention CDC Seasonal Flu Vaccine Effectiveness Studies. <https://www.cdc.gov/flu/vaccines-work/effectiveness-studies.htm>. (accessed Accessed March 11, 2022).
8. Nypaver, C.; Dehlinger, C.; Carter, C., Influenza and Influenza Vaccine: A Review. *J Midwifery Womens Health* **2021**, *66* (1), 45-53.
9. Arbeitskreis Blut, U., Influenza Virus. *Transfusion Medicine and Hemotherapy* **2009**, *36* (1), 32-39.
10. Ma, W.; García-Sastre, A.; Schwemmler, M., Expected and Unexpected Features of the Newly Discovered Bat Influenza A-like Viruses. *PLOS Pathogens* **2015**, *11* (6), e1004819.
11. Hause, B. M.; Collin, E. A.; Liu, R.; Huang, B.; Sheng, Z.; Lu, W.; Wang, D.; Nelson, E. A.;



- Li, F., Characterization of a novel influenza virus in cattle and Swine: proposal for a new genus in the Orthomyxoviridae family. *mBio* **2014**, 5 (2), e00031-14.
12. Taubenberger, J. K.; Kash, J. C., Influenza virus evolution, host adaptation, and pandemic formation. *Cell Host Microbe* **2010**, 7 (6), 440-51.
13. Medina, R. A.; García-Sastre, A., Influenza A viruses: new research developments. *Nature Reviews Microbiology* **2011**, 9 (8), 590-603.
14. Byrd-Leotis, L.; Cummings, R. D.; Steinhauer, D. A., The Interplay between the Host Receptor and Influenza Virus Hemagglutinin and Neuraminidase. *Int J Mol Sci* **2017**, 18 (7).
15. Kawaoka, Y.; Neumann, G., Influenza Viruses: An Introduction. In *Influenza Virus: Methods and Protocols*, Kawaoka, Y.; Neumann, G., Eds. Humana Press: Totowa, NJ, 2012; pp 1-9.
16. Böttcher, C.; Ludwig, K.; Herrmann, A.; van Heel, M.; Stark, H., Structure of influenza haemagglutinin at neutral and at fusogenic pH by electron cryo-microscopy. *FEBS Lett* **1999**, 463 (3), 255-9.
17. Luo, M., Influenza Virus Entry. In *Viral Molecular Machines*, Rossmann, M. G.; Rao, V. B., Eds. Springer US: Boston, MA, 2012; pp 201-221.
18. Daniels, R. S.; Downie, J. C.; Hay, A. J.; Knossow, M.; Skehel, J. J.; Wang, M. L.; Wiley, D. C., Fusion mutants of the influenza virus hemagglutinin glycoprotein. *Cell* **1985**, 40 (2), 431-439.
19. Dou, D.; Revol, R.; Ostbye, H.; Wang, H.; Daniels, R., Influenza A Virus Cell Entry, Replication, Virion Assembly and Movement. *Front Immunol* **2018**, 9, 1581.
20. Nayak, D. P.; Hui, E. K.-W.; Barman, S., Assembly and budding of influenza virus. *Virus Research* **2004**, 106 (2), 147-165.
21. Nayak, D. P.; Balogun, R. A.; Yamada, H.; Zhou, Z. H.; Barman, S., Influenza virus morphogenesis and budding. *Virus Research* **2009**, 143 (2), 147-161.
22. Palese, P.; Tobita, K.; Ueda, M.; Compans, R. W., Characterization of temperature sensitive

- 
- influenza virus mutants defective in neuraminidase. *Virology* **1974**, 61 (2), 397-410.
23. Schulze, I. T., Effects of Glycosylation on the Properties and Functions of Influenza Virus Hemagglutinin. *The Journal of Infectious Diseases* **1997**, 176 (Supplement_1), S24-S28.
24. Chen, R.; Holmes, E. C., Avian Influenza Virus Exhibits Rapid Evolutionary Dynamics. *Molecular Biology and Evolution* **2006**, 23 (12), 2336-2341.
25. U.S. Centers for Disease Control and Prevention Types of Influenza Viruses. <https://www.cdc.gov/flu/about/viruses/types.htm>. (accessed Accessed November 2, 2021.).
26. Marshall, R. D., Glycoproteins. *Annual Review of Biochemistry* **1972**, 41 (1), 673-702.
27. Gavel, Y.; Heijne, G. v., Sequence differences between glycosylated and non-glycosylated Asn-X-Thr/Ser acceptor sites: implications for protein engineering. *Protein Engineering, Design and Selection* **1990**, 3 (5), 433-442.
28. Yan, Q.; Lennarz, W. J., Oligosaccharyltransferase: A Complex Multisubunit Enzyme of the Endoplasmic Reticulum. *Biochemical and Biophysical Research Communications* **1999**, 266 (3), 684-689.
29. Yan, A.; Lennarz, W. J., Unraveling the Mechanism of Protein N-Glycosylation. *Journal of Biological Chemistry* **2005**, 280 (5), 3121-3124.
30. Kornfeld, R.; Kornfeld, S., Assembly of asparagine-linked oligosaccharides. *Annu Rev Biochem* **1985**, 54, 631-64.
31. Hubbard, S. C.; Ivatt, R. J., Synthesis and processing of asparagine-linked oligosaccharides. *Annu Rev Biochem* **1981**, 50, 555-83.
32. Wormald, M. R.; Dwek, R. A., Glycoproteins: glycan presentation and protein-fold stability. *Structure* **1999**, 7 (7), R155-R160.
33. Hebert, D. N.; Zhang, J.-X.; Chen, W.; Foellmer, B.; Helenius, A., The Number and Location of Glycans on Influenza Hemagglutinin Determine Folding and Association with Calnexin and Calreticulin. *Journal of Cell Biology* **1997**, 139 (3), 613-623.

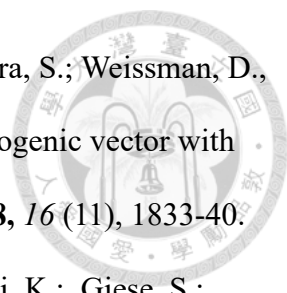
- 
34. An, Y.; McCullers, J. A.; Alymova, I.; Parsons, L. M.; Cipollo, J. F., Glycosylation Analysis of Engineered H3N2 Influenza A Virus Hemagglutinins with Sequentially Added Historically Relevant Glycosylation Sites. *Journal of Proteome Research* **2015**, *14* (9), 3957-3969.
35. Daniels, R.; Kurowski, B.; Johnson, A. E.; Hebert, D. N., N-Linked Glycans Direct the Cotranslational Folding Pathway of Influenza Hemagglutinin. *Molecular Cell* **2003**, *11* (1), 79-90.
36. Ohuchi, M.; Ohuchi, R.; Matsumoto, A., Control of biological activities of influenza virus hemagglutinin by its carbohydrate moiety. *Microbiol Immunol* **1999**, *43* (12), 1071-6.
37. Khatri, K.; Klein, J. A.; White, M. R.; Grant, O. C.; Leymarie, N.; Woods, R. J.; Hartshorn, K. L.; Zaia, J., Integrated Omics and Computational Glycobiology Reveal Structural Basis for Influenza A Virus Glycan Microheterogeneity and Host Interactions*. *Molecular & Cellular Proteomics* **2016**, *15* (6), 1895-1912.
38. Ermler Megan, E.; Kirkpatrick, E.; Sun, W.; Hai, R.; Amanat, F.; Chromikova, V.; Palese, P.; Krammer, F., Chimeric Hemagglutinin Constructs Induce Broad Protection against Influenza B Virus Challenge in the Mouse Model. *Journal of Virology* **2017**, *91* (12), e00286-17.
39. Sautto, G. A.; Kirchenbaum, G. A.; Ross, T. M., Towards a universal influenza vaccine: different approaches for one goal. *Virology* **2018**, *15* (1), 17.
40. Chen, J.; Wang, J.; Zhang, J.; Ly, H., Advances in Development and Application of Influenza Vaccines. *Front Immunol* **2021**, *12*, 711997.
41. Estrada, L. D.; Schultz-Cherry, S., Development of a Universal Influenza Vaccine. *The Journal of Immunology* **2019**, *202* (2), 392.
42. Nachbagauer, R.; Palese, P., Is a Universal Influenza Virus Vaccine Possible? *Annual Review of Medicine* **2020**, *71* (1), 315-327.
43. Paules, C. I.; Marston, H. D.; Eisinger, R. W.; Baltimore, D.; Fauci, A. S., The Pathway to a Universal Influenza Vaccine. *Immunity* **2017**, *47* (4), 599-603.



44. Ostrowsky, J.; Arpey, M.; Moore, K.; Osterholm, M.; Friede, M.; Gordon, J.; Higgins, D.; Molto-Lopez, J.; Seals, J.; Bresee, J., Tracking progress in universal influenza vaccine development. *Current Opinion in Virology* **2020**, *40*, 28-36.
45. Giles, B. M.; Ross, T. M., A computationally optimized broadly reactive antigen (COBRA) based H5N1 VLP vaccine elicits broadly reactive antibodies in mice and ferrets. *Vaccine* **2011**, *29* (16), 3043-54.
46. Zhu, X.; Han, J.; Sun, W.; Puente-Massaguer, E.; Yu, W.; Palese, P.; Krammer, F.; Ward, A. B.; Wilson, I. A., Influenza chimeric hemagglutinin structures in complex with broadly protective antibodies to the stem and trimer interface. *Proc Natl Acad Sci U S A* **2022**, *119* (21), e2200821119.
47. Nachbagauer, R.; Feser, J.; Naficy, A.; Bernstein, D. I.; Guptill, J.; Walter, E. B.; Berlanda-Scorza, F.; Stadlbauer, D.; Wilson, P. C.; Aydilto, T.; Behzadi, M. A.; Bhavsar, D.; Bliss, C.; Capuano, C.; Carreño, J. M.; Chromikova, V.; Claeys, C.; Coughlan, L.; Freyn, A. W.; Gast, C.; Javier, A.; Jiang, K.; Mariottini, C.; McMahon, M.; McNeal, M.; Solórzano, A.; Strohmeier, S.; Sun, W.; Van der Wielen, M.; Innis, B. L.; García-Sastre, A.; Palese, P.; Krammer, F., A chimeric hemagglutinin-based universal influenza virus vaccine approach induces broad and long-lasting immunity in a randomized, placebo-controlled phase I trial. *Nat Med* **2021**, *27* (1), 106-114.
48. Hai, R.; Krammer, F.; Tan, G. S.; Pica, N.; Eggink, D.; Maamary, J.; Margine, I.; Albrecht, R. A.; Palese, P., Influenza viruses expressing chimeric hemagglutinins: globular head and stalk domains derived from different subtypes. *J Virol* **2012**, *86* (10), 5774-81.
49. Liao, H.-Y.; Wang, S.-C.; Ko, Y.-A.; Lin, K.-I.; Ma, C.; Cheng, T.-J. R.; Wong, C.-H., Chimeric hemagglutinin vaccine elicits broadly protective CD4 and CD8 T cell responses against multiple influenza strains and subtypes. *Proceedings of the National Academy of Sciences* **2020**, *117* (30), 17757-17763.



50. Meier, S.; Güthe, S.; Kiefhaber, T.; Grzesiek, S., Foldon, The Natural Trimerization Domain of T4 Fibrin, Dissociates into a Monomeric A-state Form containing a Stable β -Hairpin: Atomic Details of Trimer Dissociation and Local β -Hairpin Stability from Residual Dipolar Couplings. *Journal of Molecular Biology* **2004**, *344* (4), 1051-1069.
51. Petrovsky, N.; Aguilar, J. C., Vaccine adjuvants: Current state and future trends. *Immunology & Cell Biology* **2004**, *82* (5), 488-496.
52. Pardi, N.; Hogan, M. J.; Porter, F. W.; Weissman, D., mRNA vaccines — a new era in vaccinology. *Nature Reviews Drug Discovery* **2018**, *17* (4), 261-279.
53. Tseng, Y. C.; Wu, C. Y.; Liu, M. L.; Chen, T. H.; Chiang, W. L.; Yu, Y. H.; Jan, J. T.; Lin, K. I.; Wong, C. H.; Ma, C., Egg-based influenza split virus vaccine with monoglycosylation induces cross-strain protection against influenza virus infections. *Proc Natl Acad Sci U S A* **2019**, *116* (10), 4200-4205.
54. Chen, J. R.; Yu, Y. H.; Tseng, Y. C.; Chiang, W. L.; Chiang, M. F.; Ko, Y. A.; Chiu, Y. K.; Ma, H. H.; Wu, C. Y.; Jan, J. T.; Lin, K. I.; Ma, C.; Wong, C. H., Vaccination of monoglycosylated hemagglutinin induces cross-strain protection against influenza virus infections. *Proc Natl Acad Sci U S A* **2014**, *111* (7), 2476-81.
55. Wu, C. Y.; Cheng, C. W.; Kung, C. C.; Liao, K. S.; Jan, J. T.; Ma, C.; Wong, C. H., Glycosite-deleted mRNA of SARS-CoV-2 spike protein as a broad-spectrum vaccine. *Proc Natl Acad Sci U S A* **2022**, *119* (9).
56. Hou, X.; Zaks, T.; Langer, R.; Dong, Y., Lipid nanoparticles for mRNA delivery. *Nature Reviews Materials* **2021**, *6* (12), 1078-1094.
57. Pardi, N.; Tuyishime, S.; Muramatsu, H.; Kariko, K.; Mui, B. L.; Tam, Y. K.; Madden, T. D.; Hope, M. J.; Weissman, D., Expression kinetics of nucleoside-modified mRNA delivered in lipid nanoparticles to mice by various routes. *Journal of Controlled Release* **2015**, *217*, 345-351.



58. Karikó, K.; Muramatsu, H.; Welsh, F. A.; Ludwig, J.; Kato, H.; Akira, S.; Weissman, D., Incorporation of pseudouridine into mRNA yields superior nonimmunogenic vector with increased translational capacity and biological stability. *Mol Ther* **2008**, *16* (11), 1833-40.
59. Oberhardt, V.; Luxenburger, H.; Kemming, J.; Schulien, I.; Ciminski, K.; Giese, S.; Csernalabics, B.; Lang-Meli, J.; Janowska, I.; Staniek, J.; Wild, K.; Basho, K.; Marinescu, M. S.; Fuchs, J.; Topfstedt, F.; Janda, A.; Sogukpinar, O.; Hilger, H.; Stete, K.; Emmerich, F.; Bengsch, B.; Waller, C. F.; Rieg, S.; Sagar; Boettler, T.; Zoldan, K.; Kochs, G.; Schwemmler, M.; Rizzi, M.; Thimme, R.; Neumann-Haefelin, C.; Hofmann, M., Rapid and stable mobilization of CD8⁺ T cells by SARS-CoV-2 mRNA vaccine. *Nature* **2021**, *597* (7875), 268-273.
60. Karikó, K.; Muramatsu, H.; Welsh, F. A.; Ludwig, J.; Kato, H.; Akira, S.; Weissman, D., Incorporation of Pseudouridine Into mRNA Yields Superior Nonimmunogenic Vector With Increased Translational Capacity and Biological Stability. *Molecular Therapy* **2008**, *16* (11), 1833-1840.

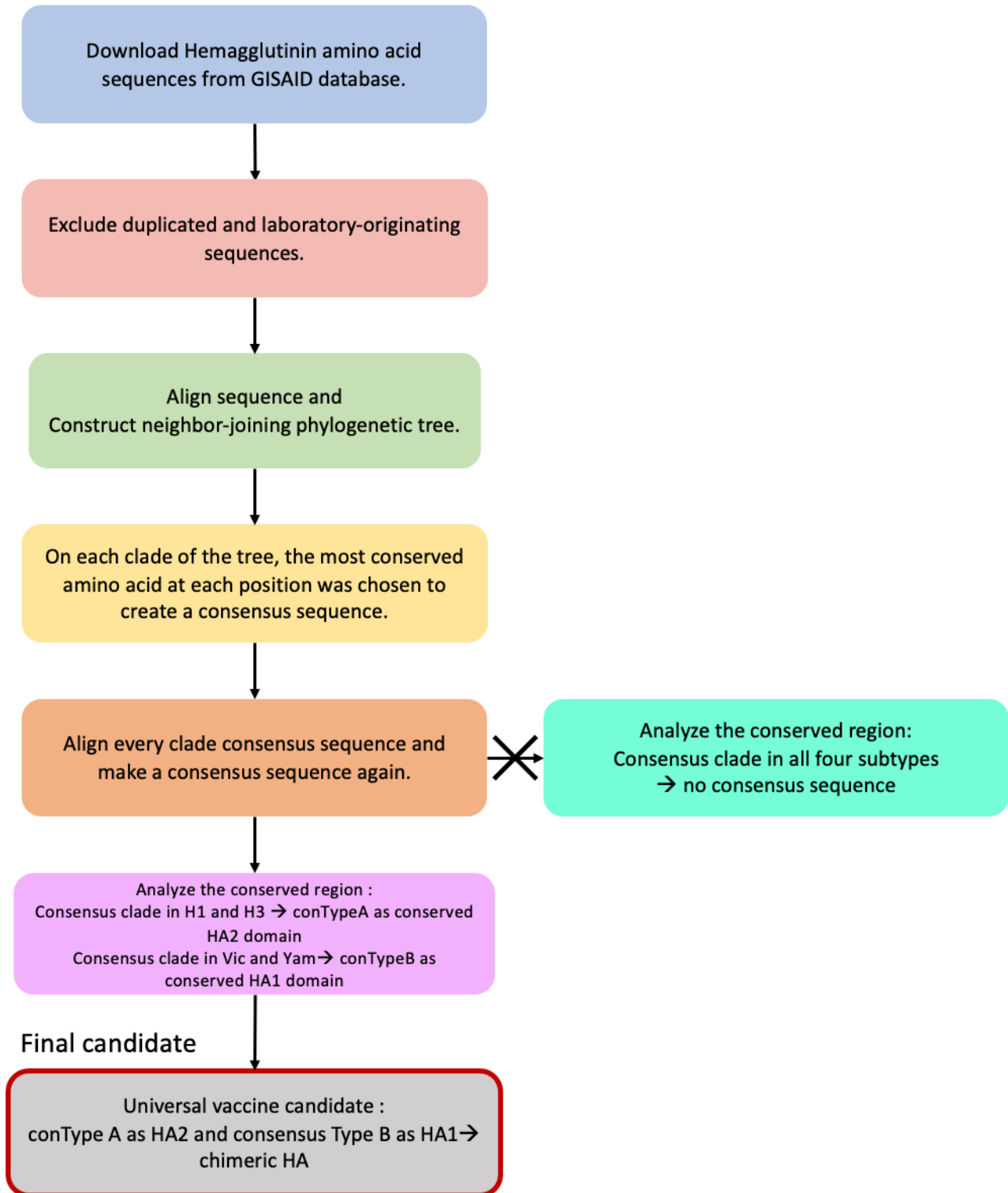


Figure 1. The workflow of chimeric HA design.

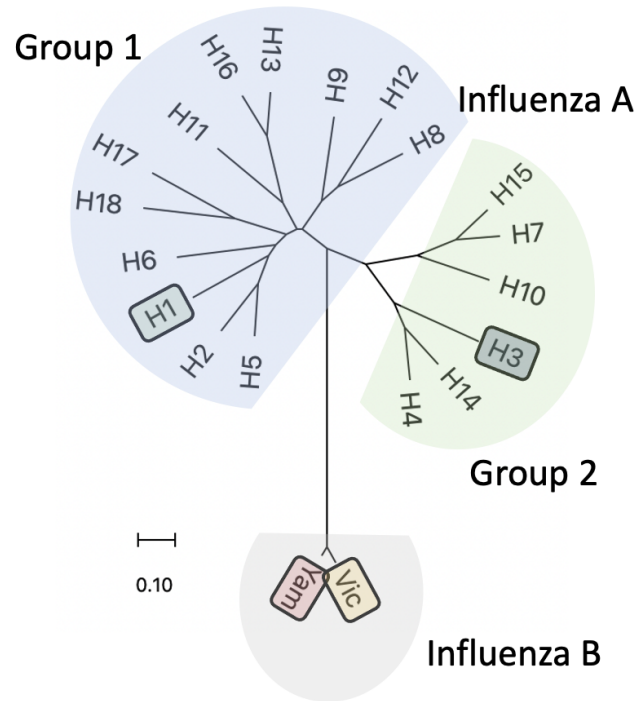
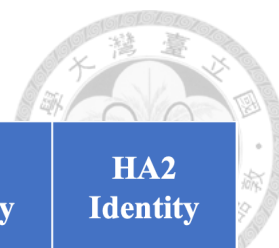


Figure 2. The phylogenetic tree of HA subtypes that were constructed with HA sequences extracted from GISAID database by MEGA 11 software.

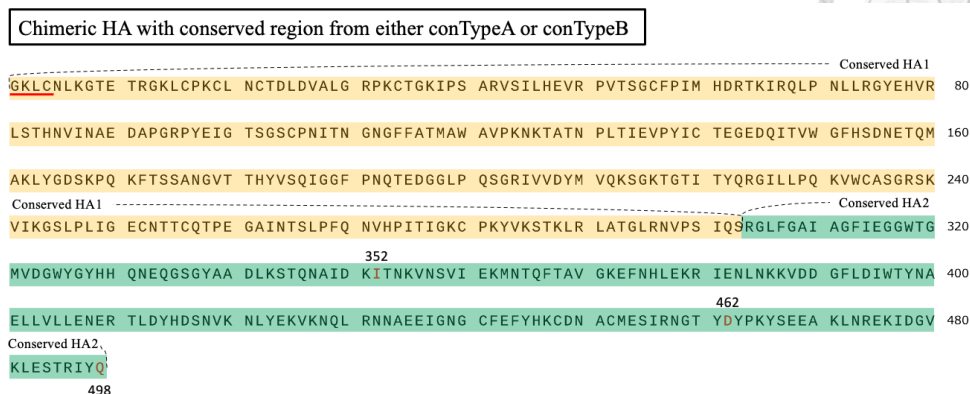


	Subtypes or Lineages	Sequences Number	Full Length Identity	HA1 Identity	HA2 Identity
Influenza A	H1	61,655	40%	31%	65%
	H3	75,423			
Influenza B	Yamgata	17,174	92%	88%	98%
	Victoria	21,891			

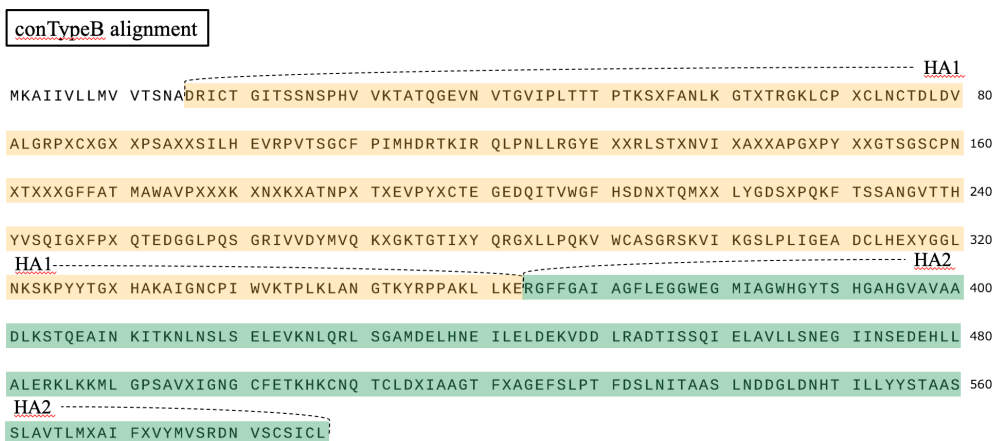
Figure 3. Sequence comparison of HA sequences obtained from GISAID database and used for cHA design.



(A)



(B)



(C)

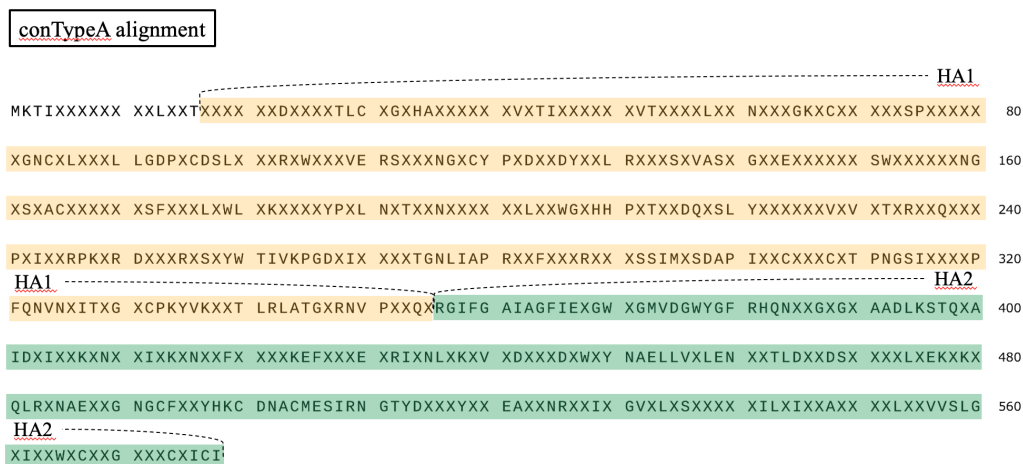
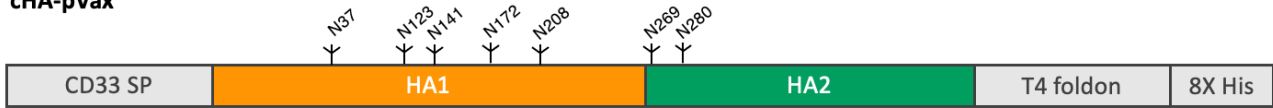


Figure 4. The proteins sequences of chimeric HA (A), Consensus type B (B) and Consensus type A (C). X represented non-conserved amino acid sites.



(A)

cHA-pVax



(B)

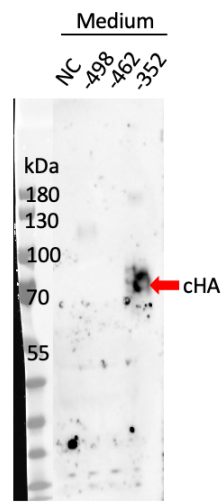


Figure 5. The design and expression of recombinant cHA proteins.

(A) The construction of cHA-pVax1 expression plasmid. Seven predicted N-glycosylation sites were marked. SP represented signal peptides. (B) Expression of full-length cHA (cHA-498) and C-terminal truncated cHA (cHA-462 and cHA-352) in HEK293T cells. HEK293T cells were transfected indicated expression plasmids and the secreted medium were collected after 48 hours. The medium were processed for immunoblotting analysis by using anti-His-HRP antibodies to detect the cHA expression. NC represented negative control.



cHA	-----GKLCNLKGTETRGKLCPKCLNCTDLD	26
conTypeA	MKTIXXXXXXXXLXXTXXXXXXXXDXXXTLCXGXHAXXXXXXXXXVXTIXXXXXXXXVTXXXXLXXNXXGKXCXXXXXSP--XXXXXXXXGNCXLXX	88
conTypeB	MKAIIVL-----LMVVTSNADRICTGITSSNSPHVVKTATQGEVNVTVGIPLTTTTPTKSXFANLKGXTTRGKLCPCXCLNCTDLD	79
cHA	VALGRPKCTGKIPSARVSI-LHEVRPVTSGCFPIIMHDRTKIRQLPNLLRGYEHVRLSTHNVINAE-----DAPGRPYEIGTSGSCP	106
conTypeA	XLLGDPXCDSLXXXRXWXXXVERSXXXNGXCYPDXD-----YXXLRXXXSVASXGXEXXXXXXSWXXXXXXXXNXSXCX	166
conTypeB	VALGRPCXCGXXPSAXXSI-LHEVRPVTSGCFPIIMHDRTKIRQLPNLLRGYEXXRLSTXNVIXAX-----XAPGXPYXGTSGSCP	159
cHA	NITNGNGFFATMAWAVPKN-----KTATNPLTIEVPYICTEGEDQITVWGFHSDNETQ-MAKLYGDSKPQKFTSSANGVTTHYVSQIGGF	190
conTypeA	XX-XXXSFXXLXWLNKXXXXYPX-----LNXTXXNXXXXXXXXLXXWGXHHPXTXXDQXSLYXXXXXXXXVXTX-RXXQXXXPIXXR	246
conTypeB	NXTXXGFFATMAWAVPXXXKXNXKXATNPXTXEVYXCTEGEDQITVWGFHSDNXTQ-MXXLYGDSXPQKFTSSANGVTTHYVSQIGXF	248
cHA	PNQTEDGGLPQSGRIVVDYVMVQKSGKTGTITYQRGILLPQKVVCA-SGRSKVIKGSPLLIGECNTTCQTPEGAINSTLPPFNVPITIGK	279
conTypeA	PKXRD-----XXXRXSYWTIVKPGDXIXXXTGNLIAPRXXFXXRXSSIMXSDAPIXXCXXXCXTPEGAIXXXPFQNVHXITXGX	331
conTypeB	PXQTEDGGLPQSGRIVVDYVMVQKXGKTGTIXYQRGXLLPQKVVCA-SGRSKVIKGSPLLIGEDCLHEXYGGLNKSXPYYTGXHAKAIGN	337
cHA	CPKYVKSTKLRRLATGLRNVP---SIQSRGLFGAIAGFIEGGWTGMVDGWYGYHHQNEQSGYAADLKSTQNAIDKI-----	352
conTypeA	CPKYVKXXKLRRLATGXRNV---XXQXRGLFGAIAGFIEGXGMDGWYGYHHQNXGXGXAADLKSTQXAIIXXKXNXXIXKXNXX	418
conTypeB	CPIWVKTP-LKLANGTKYRPPAKLLKERGFAGIAGFLEGGWEGMIAGWHGYTSHGAHGVAAADLKSTQEAINKITKNLSLSELEVKN	426
cHA	-----	
conTypeA	FXXXXKEFXXEXRINLXKXVXDXXDXWYNAELLVXLENXTLDXXDSXXXXLXEKXXQLRXNAEXXGNGCFXYHKCDNACMESI	352
conTypeB	LQRLSGAMDELHNEILELDEKVDDLADTISSQIELAVLLSNEGIINSEDEHLLALERKLLKMLGPSAVXIGNGCFETKHKCNQTCLDXI	516
cHA	-----	
conTypeA	RNGTYDXXYXXEAXNRXXIXGVXLXS--XXXXXILXIXAXXXLXXVSLGXIXXWXCXXGXXXCXICI	352
conTypeB	AAGTFXAGEFSLPTFDLSLNI-TAASLNDGDLNHTILLYYSTAASSLAVTLMXAIFXVYVMSRDNVSCSICL	578
		587

Figure 6. The final sequence of chimeric HA used in this study. The cHA352 was aligned with conTypeA and conTypeB.

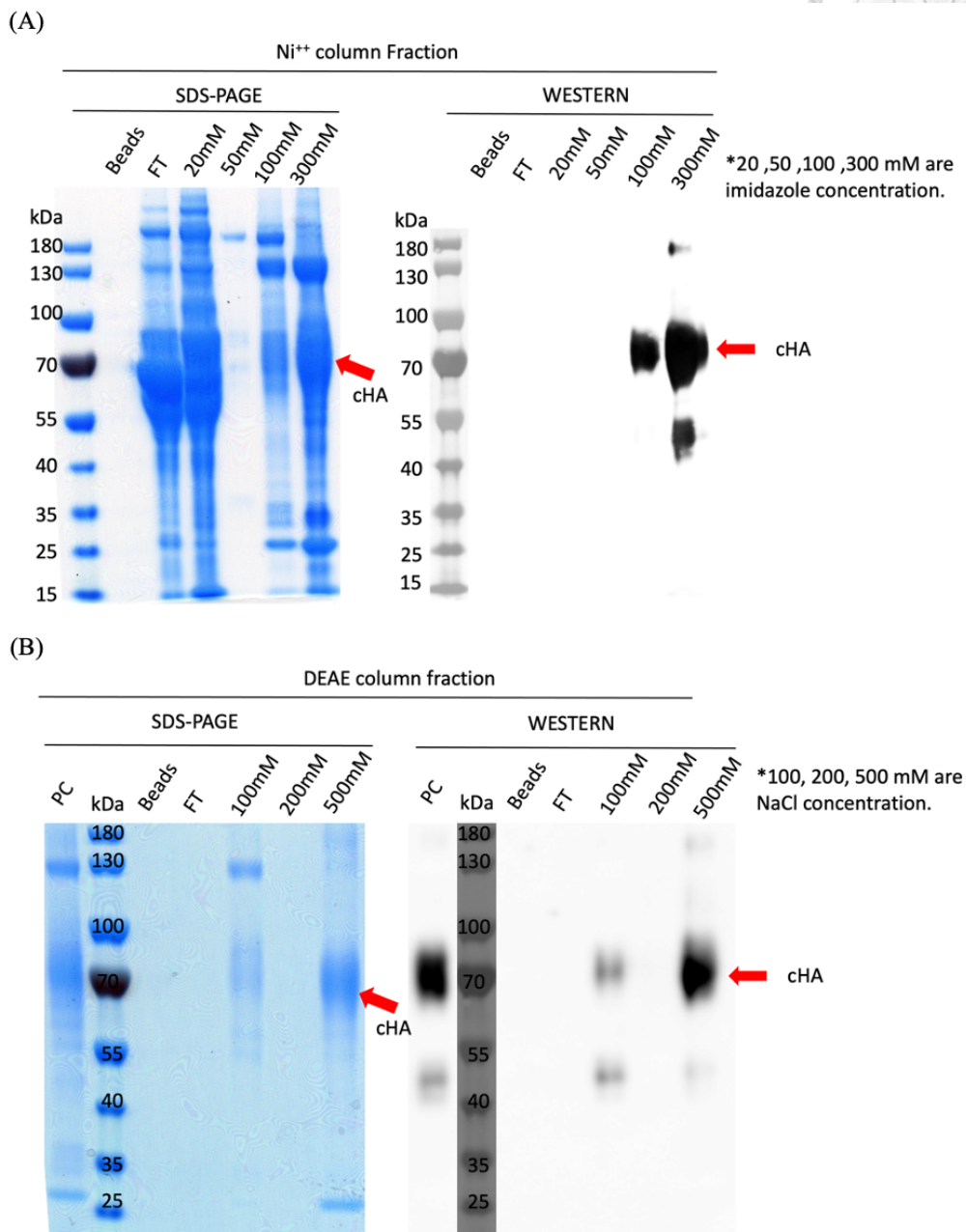


Figure 7. Purification of cHA with Ni⁺⁺ Sepharose chromatography and DEAE Sepharose chromatography.

(A) SDS-PAGE and western blotting of the fractions from Ni⁺⁺ column. (B) SDS-PAGE and western blotting of the fractions from DEAE column. Mouse anti-His primary antibody and secondary anti-mouse-HRP antibody used to detect cHA signal.



MPLLLLPLIIVAGALAGKLCNLKGTETRGKLCPKCLNCTDLDV¹⁰ALGRPKCTGKIPSA²⁰R³⁰VSILHEVRPVTSGCFPIMHDRTKIRQLPNLLRGYEHVRLSTH⁴⁰
NVINAEDAPGRPYEIGTSGSCPNITNGNGFFATMA¹¹⁰WAVPKNKTATNPLTIEVPYICTEGEDQITVWGFHSDNETQMAKLYGDSKPKFTSSANGVTTHYV¹²⁰
SQIGGFNPQTEDGGLPQSGRIVVDYMWQKSGKTGTITTYQRGILLPQKVWCASGRSKVIK¹³⁰GSPLIGE¹⁴⁰CNTTCQTP¹⁵⁰EGAIN¹⁶⁰TSLPFQNVHPITIGKCPKYV¹⁷⁰
KSTKLRLATGLRNVPSIQSRG²¹⁰LF²²⁰GAIAG²³⁰FI²⁴⁰EGG²⁵⁰WTGM²⁶⁰V²⁷⁰DG²⁸⁰WYGYHHQNEQSGYAADLKSTQNAIDKILVPRGSPGSGYIPEAPRDGQAYVVRKDGEWVLL³¹⁰
³²⁰STFLGHHHHHHHH⁴⁰⁰

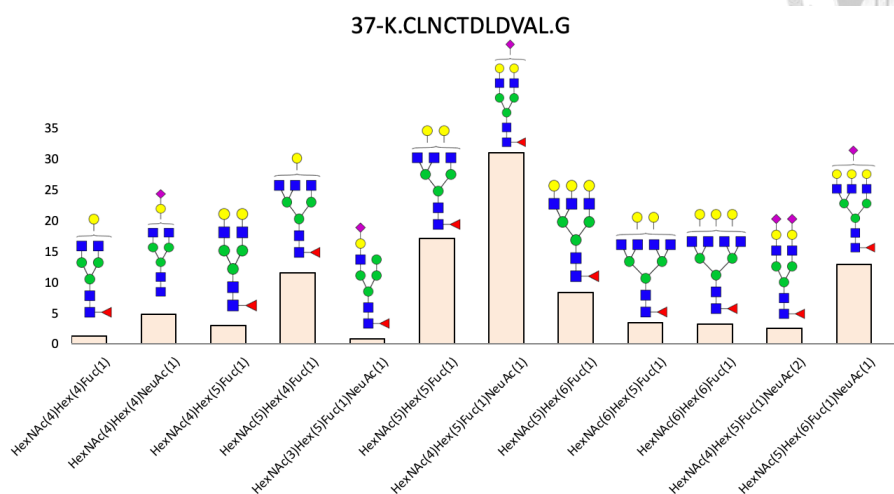
Figure 8. Protein identification of cHA by LC-MS/MS analysis.

Protein identification of the protein bands corresponding to the 70kDa band shown in Figure 7.

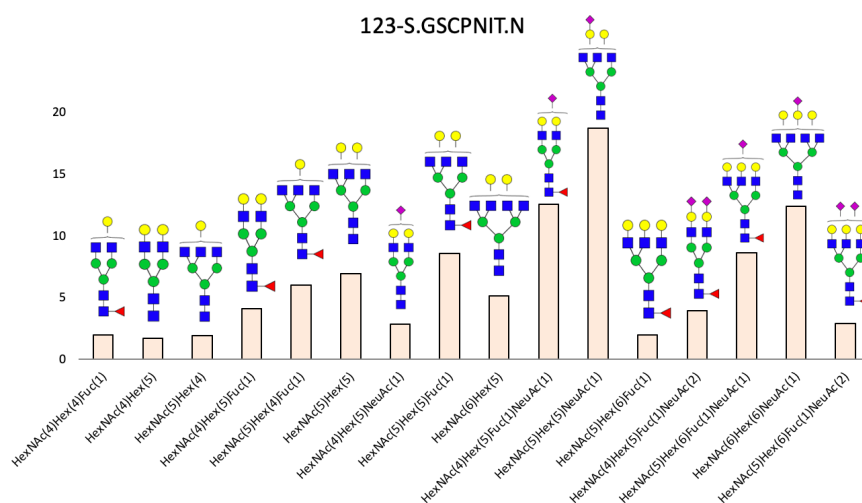
Found peptides were underlined.



(A)



(B)



(C)

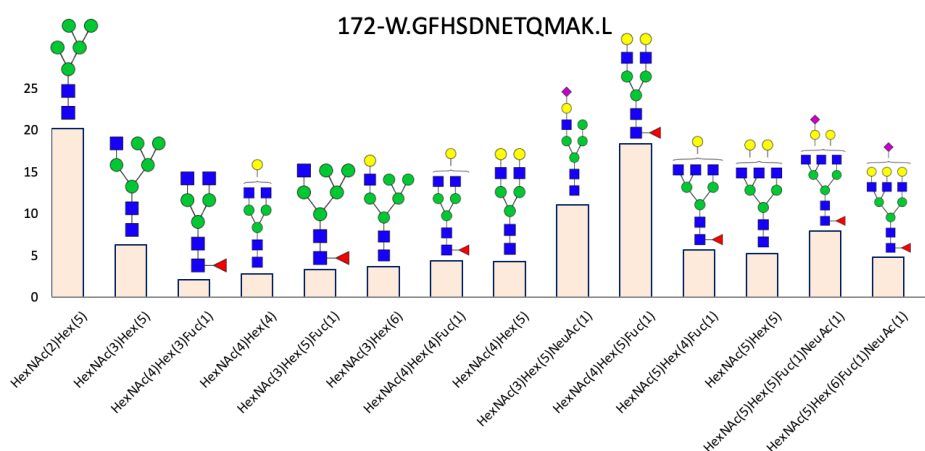
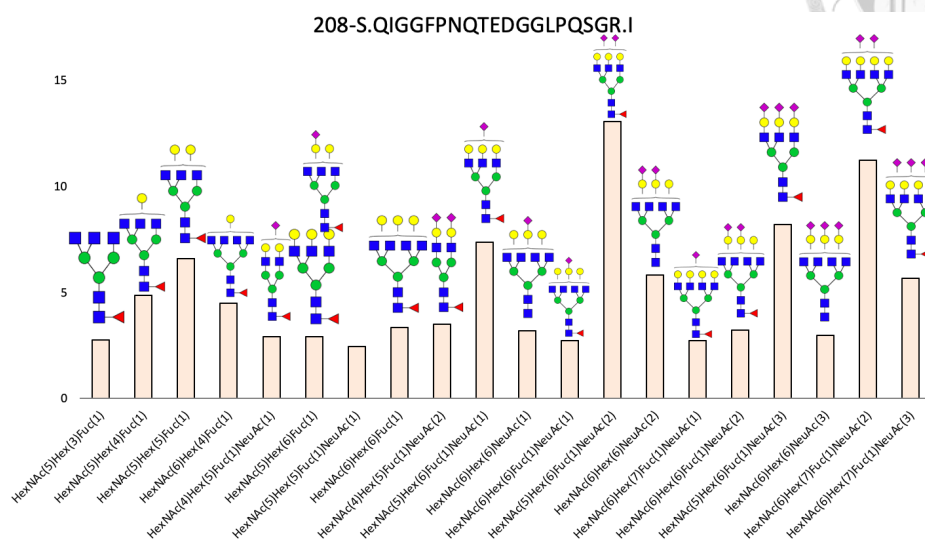


Figure 9. Continued



(D)



(E)

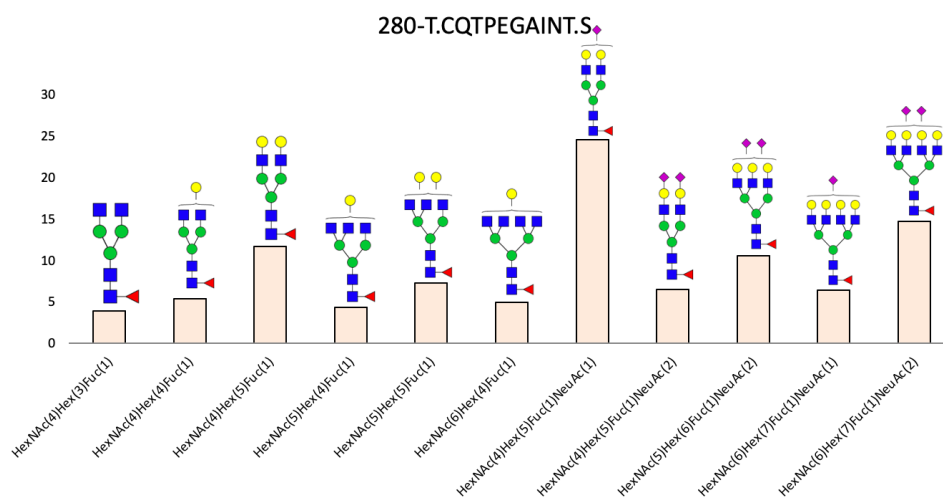
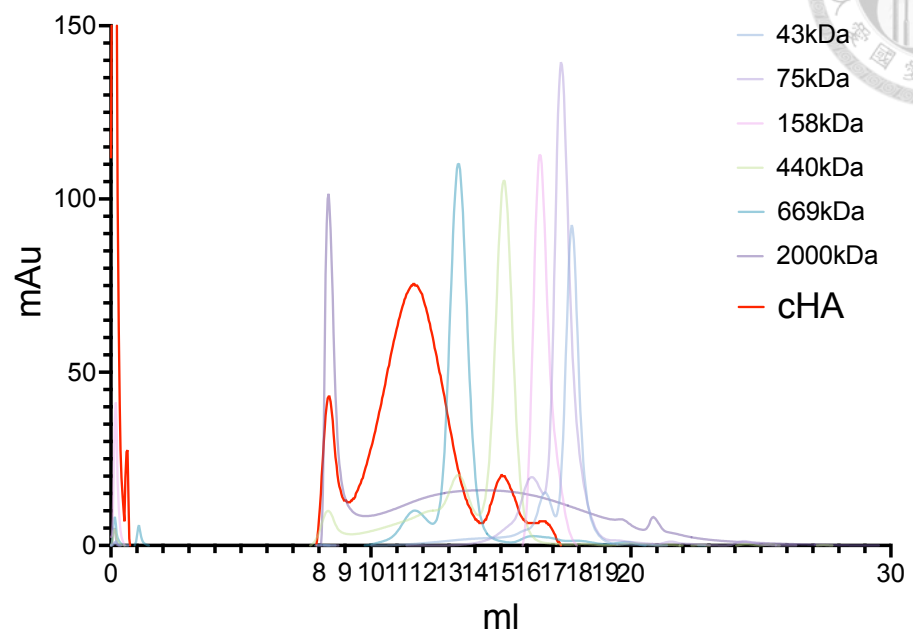


Figure 9. Glycan-profiling of cHA by LC-MS/MS.

The cHA proteins were digested with trypsin, chymotrypsin and α -lytic protease and processed for glycan profiling by LC-MS/MS analysis. Blue square: GlcNAc. Green circle: Man. Yellow circle: Gal. Purple diamond: Sialic acid. Red triangle: Fuc.



(A)



(B)

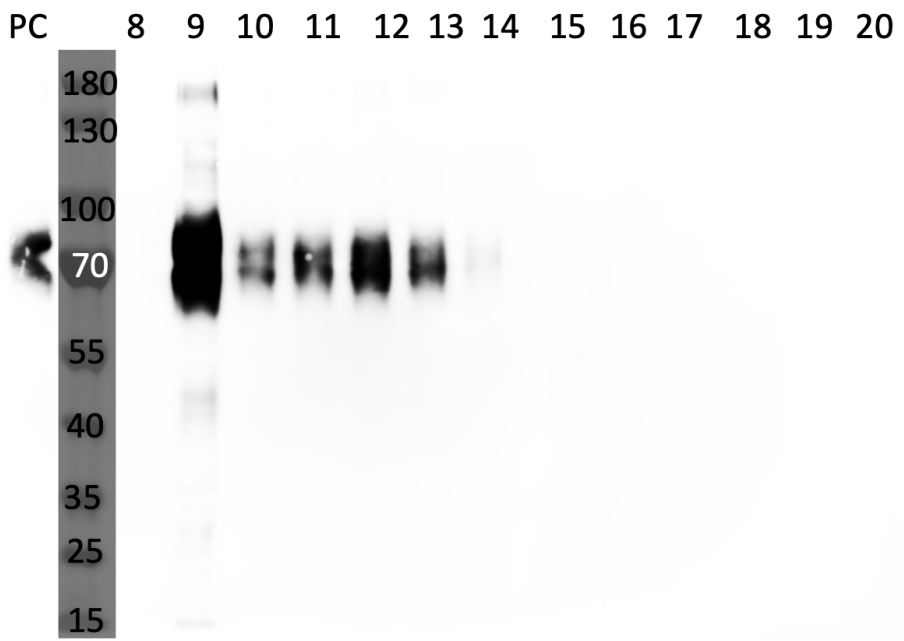


Figure 10. cHA protein characterization by size exclusion chromatography.

(A) The elution profiles of cHA and standard proteins on SEC. Red line represents cHA protein. (B) The eluted fractions were collected and processed for immunoblotting analysis. The immunoblotting of SEC fractions. PC represents positive control, which is cHA from anion exchange purification and before loaded onto the SEC.

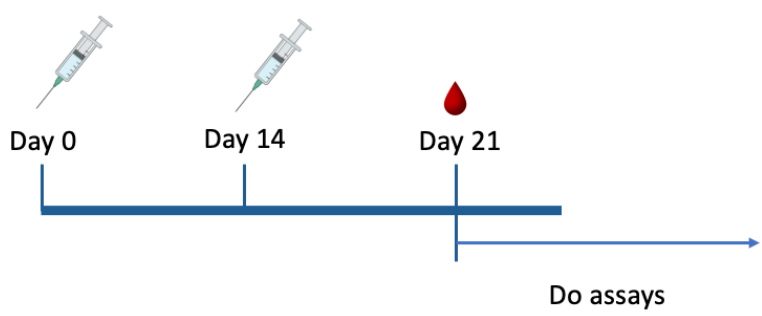


(A)

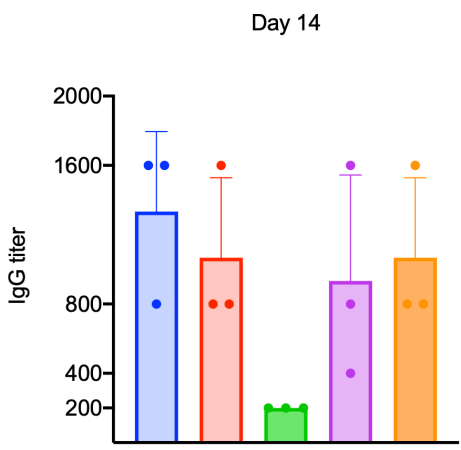


BALB/c
6-8 weeks
N=3

Group (n=3)		
1	Negative control	endotoxin-free water
2	cHA protein	20ug+ 50ug adjuvant



(B)



(C)

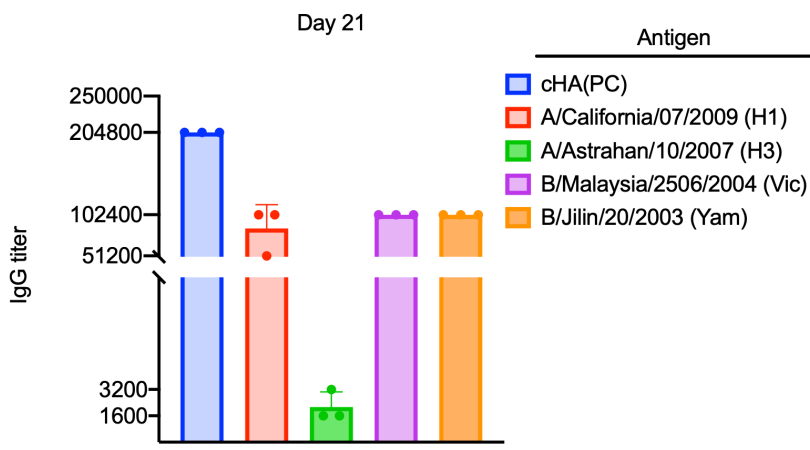


Figure 11. Animal experiment time-line and immunogenicity of cHA.

(A) Mice vaccination experiment design. (B) and (C) The ELISA endpoint titer assay of serum collected at Day 14 and Day 21. Different subtype of HA proteins were used as the coating proteins to assess serum IgG titer. Y axis represented serum dilution titer.

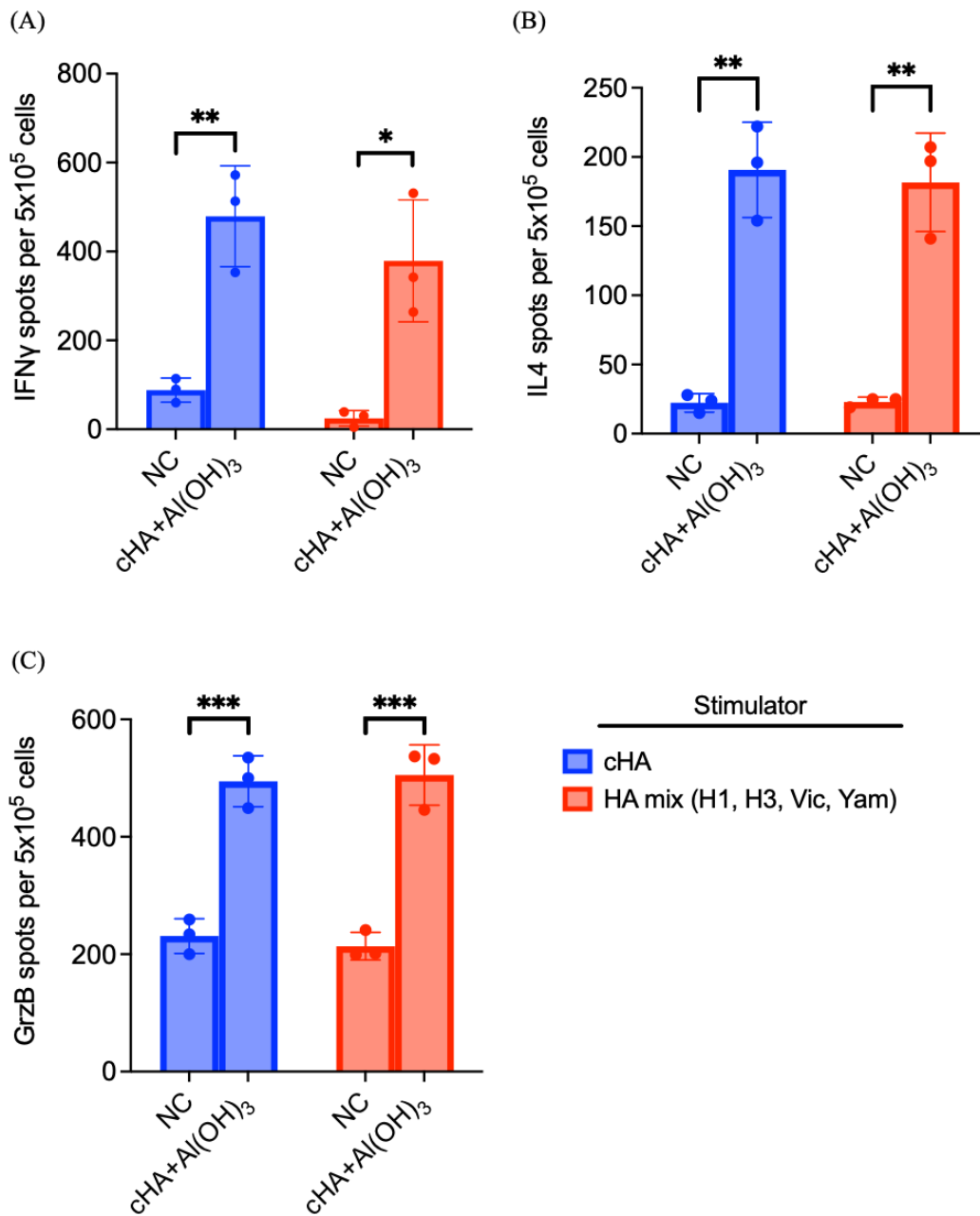
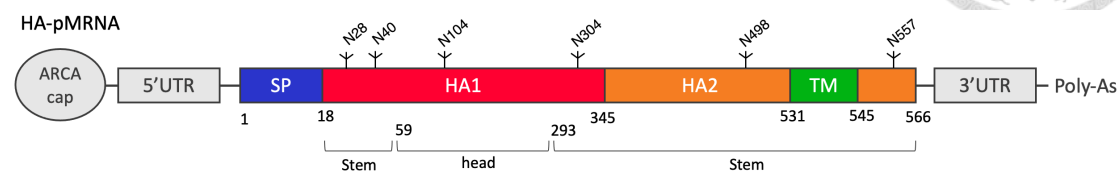


Figure 12. ELISpot analysis of splenocytes from cHA immunized mice.

(A) IFN γ , (B) IL4 and (C) GrzB spots per 5×10^5 splenocytes were measured by ELISpot with two different protein stimulators (cHA and HA mix of H1, H3, Vic and Yam). Symbols represent individual mice. Heights of bars indicate the mean. P values compare cHA protein groups with the negative control (parametric, two-tailed paired t-test).



(A)



(B)

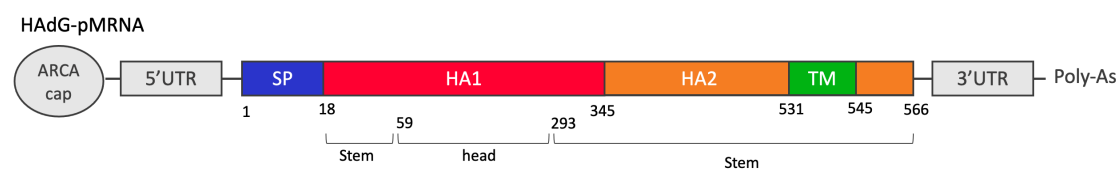
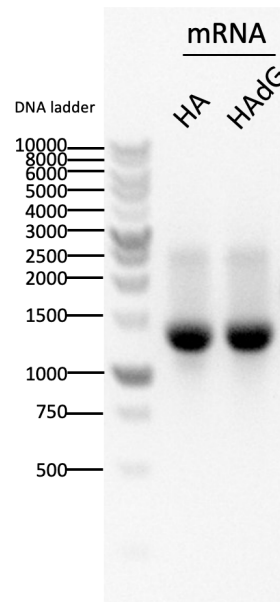


Figure 13. mRNA synthesis constructions.

(A) Diagram of A/Cal/07/2009 H1N1 HA in pMRNA vector. (B) Diagram of A/Cal/07/2009 H1N1 HA without N-glycosites in pMRNA vector. ARCA represented anti-reverse cap analog [m7G(5')ppp(5')G].



(A)



(B)

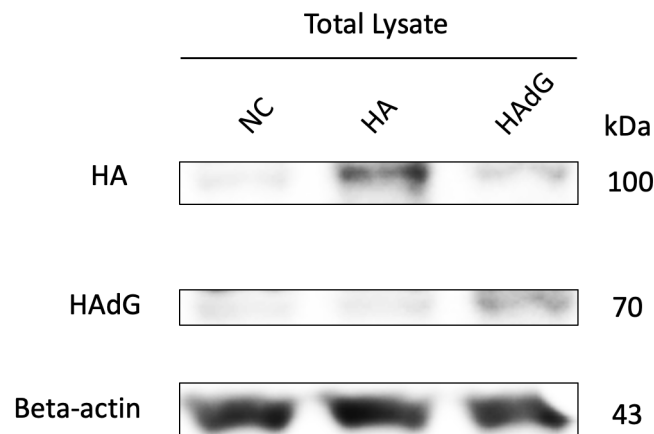


Figure 14. Agarose gel of in vitro transcribed mRNA and western blotting of mRNA transfected cells.

(A) Agarose gel of mRNA transcribed from HA-pMRNA and HAdG-pMRNA. (B) The western blotting of HA and HAdG in the mRNA-transfected HEK293T cells. HEK293T cells were transfected with mRNA and the cell lysates were prepared and processed for immunoblotting analysis. Primary goat anti-HA specific antibody and secondary anti-goat-HRP antibody are used to detect specific HA signal.



(A)

```
>HA
MKAILVLLYTFATANADTLCIGYHANNSTDTVDTVLEKNVTVTHSVNLEDKHNGKLCCLRGVAPLHLGKCNIAGWILGNPECESLSTASSWSYIVE
TPSSDNGTCYPGDFIDYEELREQLSSVSSFERFEIFPKTSSWPNHDSNKGVTAACPHAGAKSFYKNLIWLVKGNSYPKLSKSYINDKGKEVLVLWGIH
HPSTSADQQSLYQNADAYVFGSSRYSKFKPEIAIRPKVRDQEGRMNYYWTLVEPGDKITFEATGNLVVPRYAFAMERNAGSGIISDTPVHDCNT
TCQTPKGAINSLPFQNIHPITIGKCPKYVKSTKLRLATGLRNIPSIQSRGLFGAIAAGFIEGGWTGMVDGWYGYHHQNEQSGGYAADLKSTQNAIDEI
TNKVNSVIEKMNTQFTAVGKEFNHLEKRIENLNKKVDDGFLDIWYNAELLVLENERLDYHDSNVKNLYEKVRSQKNNAKEIGNGCFEFYHKCD
NTCMESVKNGTYDYPKYSEEAKLNREEIDGVKLESTRIYQILAIYSTVASSLVLVSLGAISFWMCSNGSLQCRICI
```

(B)

```
>HAdG
MKAILVLLYTFATANADTLCIGYHANQSTDTVDTVLEKQVTVTHSVNLEDKHNGKLCCLRGVAPLHLGKCNIAGWILGNPECESLSTASSWSYIVE
TPSSDQGTCTYPGDFIDYEELREQLSSVSSFERFEIFPKTSSWPNHDSNKGVTAACPHAGAKSFYKNLIWLVKGNSYPKLSKSYINDKGKEVLVLWGIH
HPSTSADQQSLYQNADAYVFGSSRYSKFKPEIAIRPKVRDQEGRMNYYWTLVEPGDKITFEATGNLVVPRYAFAMERNAGSGIISDTPVHDCNT
TCQTPKGAIQTSPLPFQNIHPITIGKCPKYVKSTKLRLATGLRNIPSIQSRGLFGAIAAGFIEGGWTGMVDGWYGYHHQNEQSGGYAADLKSTQNAIDEI
TNKVNSVIEKMNTQFTAVGKEFNHLEKRIENLNKKVDDGFLDIWYNAELLVLENERLDYHDSNVKNLYEKVRSQKNNAKEIGNGCFEFYHKCD
NTCMESVKQGTYPKYSEEAKLNREEIDGVKLESTRIYQILAIYSTVASSLVLVSLGAISFWMCSQGSQSLQCRICI
```

Figure 15. Protein identification of mRNA translated HA and HAdG protein by LC-MS/MS analysis.

(A) Protein identification of the protein bands corresponding to the 100 kDa band shown in Figure 13B, and (B) Protein identification of the protein bands corresponding to the 70 kDa band shown in Figure 13B. Found peptides were marked in red.

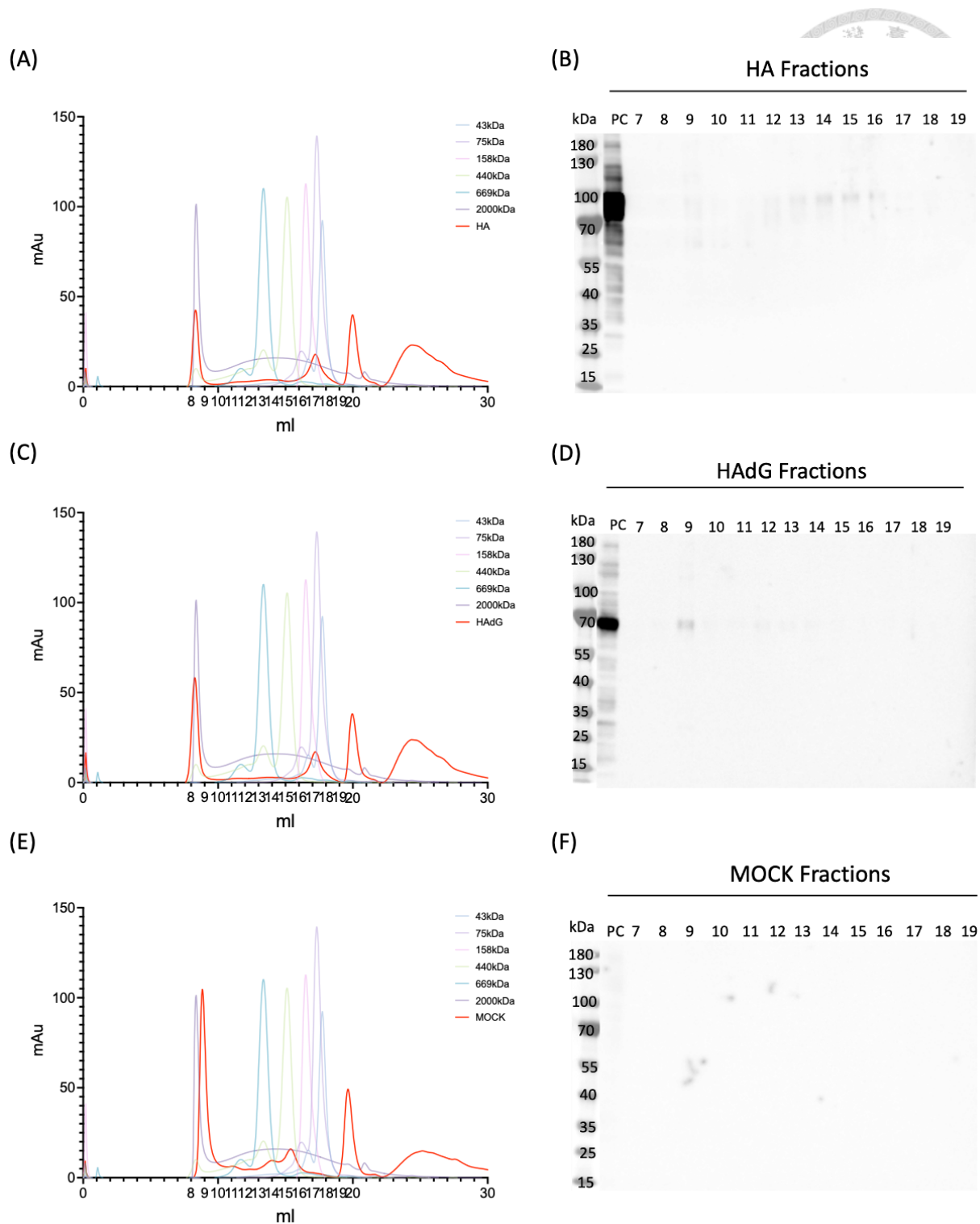


Figure 16. Size exclusion chromatography of HA and HAdG expressed in HEK293T cells. (A), (C), (E) The SEC profile of HA mRNA, HAdG mRNA or MOCK transfected HEK293T lysate. (B), (D), (F) are the western blotting of SEC fractions. MOCK is empty vector. PC is cell lysate before loaded onto SEC. Primary goat anti-HA specific antibody and secondary anti-goat-HRP antibody are used to detect specific HA signal.

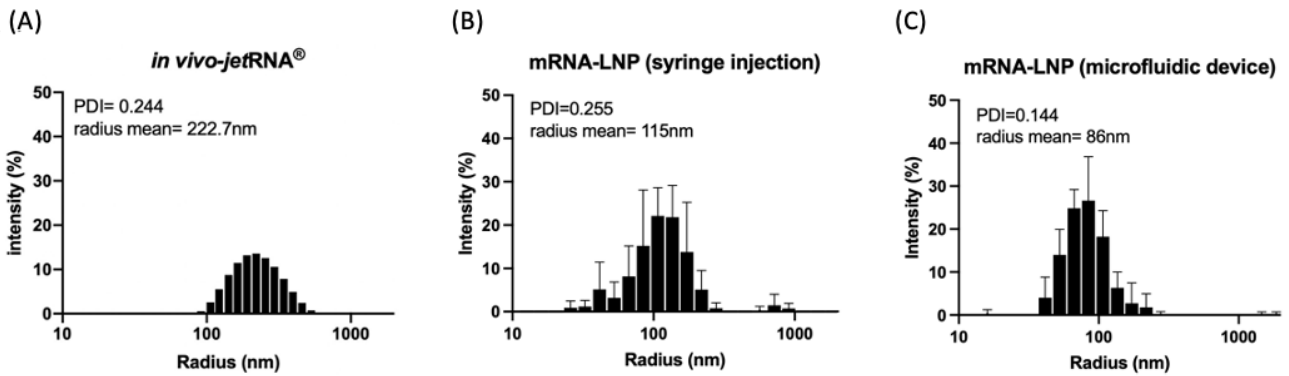


Figure 17. Size distribution of prepared mRNA-Lipid nanoparticle.

mRNA-lipid nanoparticles were prepared with In vivo jet (A), a combination of four lipids with manual injection (B) and a combination of four lipids with a microfluidic device (C). The prepared mRNA-LNPs were collected and subjected for dynamic light scattering analysis. PDI (polydispersity index) and measured particle sizes were shown.

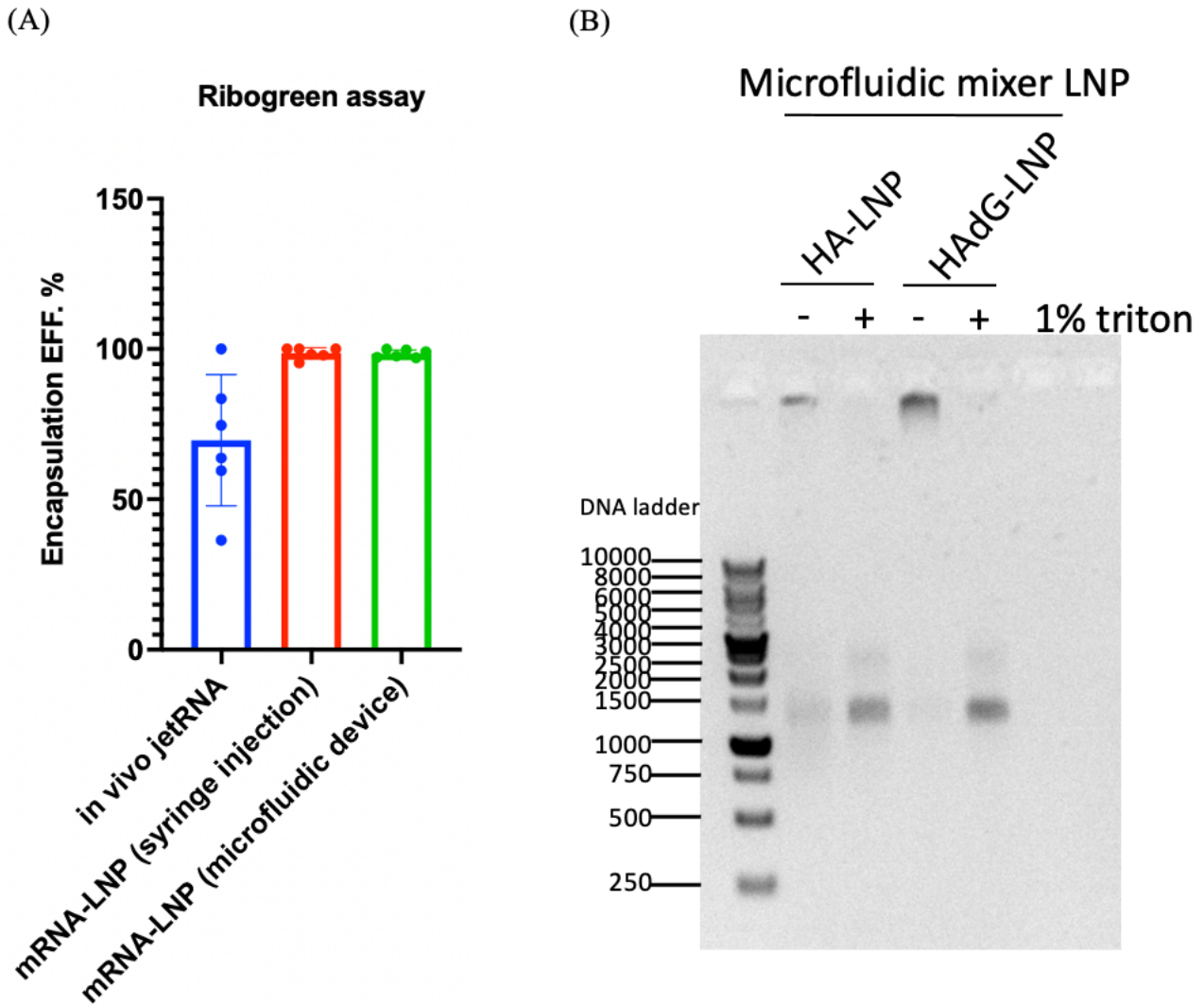


Figure 18. Encapsulation efficiency of mRNA-Lipid nanoparticle.

(A) Ribogreen assay for quantification of mRNA encapsulation efficiency. Bars represent groups mean \pm SD (n=6). (B) mRNA-LNP were incubated with or without Triton X-100. The reactions were then processed for agarose gel analysis.

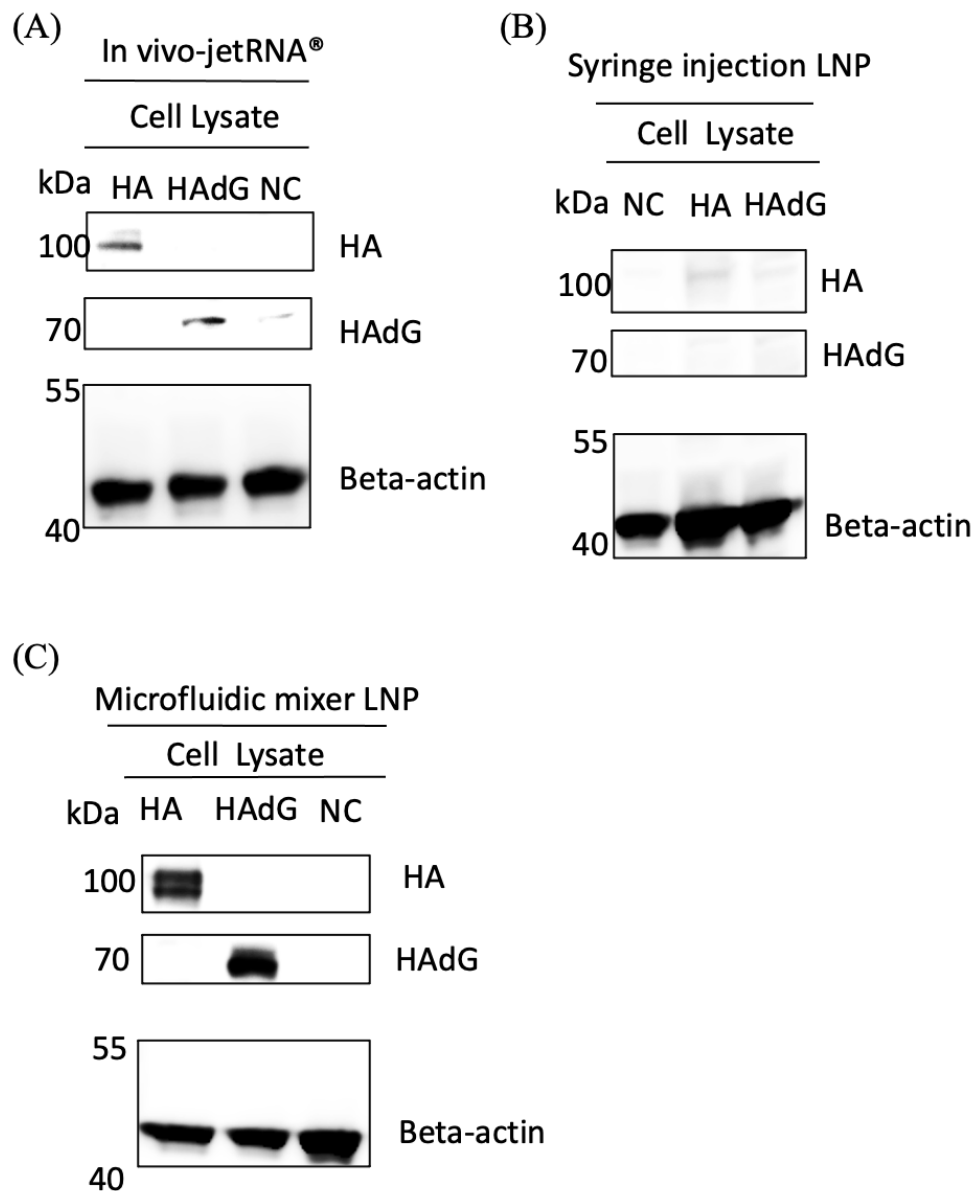
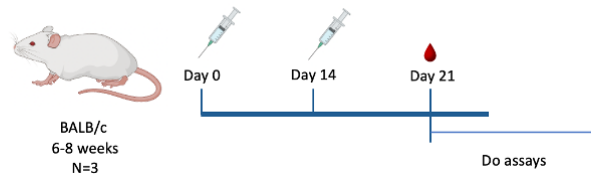


Figure 19. HA expression in mRNA-LNP transfected cells. HEK293T cells were transfected with mRNA mixed with In vivo-jet (A), mRNA-LNP (B, C) and the cells were collected for immunoblotting analysis. NC is negative control. Primary goat anti-HA specific antibody and secondary anti-goat-HRP antibody were used to detect specific HA signal.

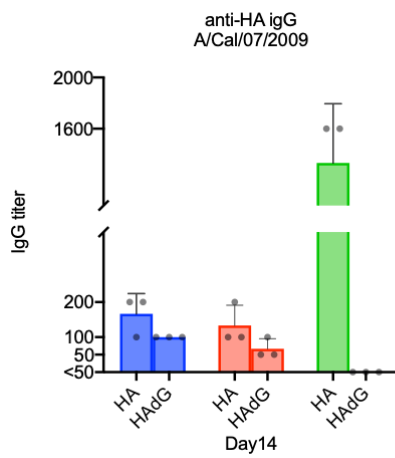


(A)

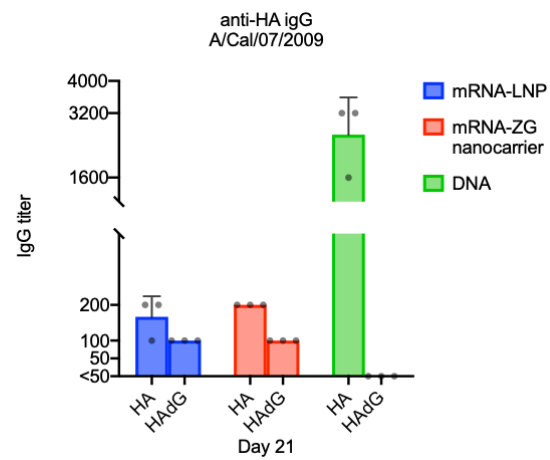


Group (n=3)		
1	Negative control	endotoxin-free water
2	Positive control (HA and HAdG DNA)	100 ug per dose
3	HA mRNA-LNP	5 ug per dose
4	HAdG mRNA-LNP	5 ug per dose
5	HA mRNA-ZG nanocarrier	5 ug per dose
6	HAdG mRNA-ZG nanocarrier	5 ug per dose

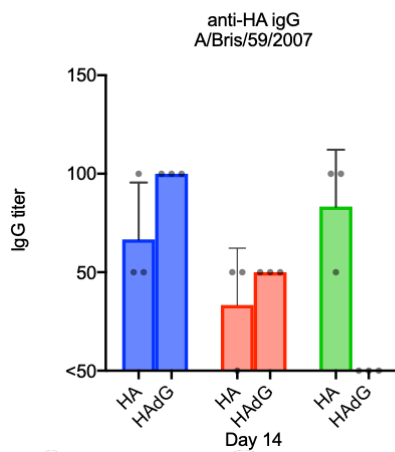
(B)



(C)



(D)



(E)

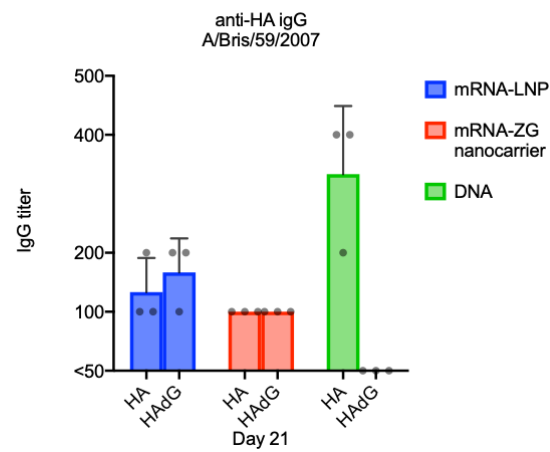


Figure 20. Animal experiment time line and immunogenicity of HA and HAdG nucleotides vaccine.

(A) Mice vaccination experiment design. (B) and (C) ELISA endpoint titer assay using the serum at Day 14 and Day 21. A/Cal/07/2009 and A/Bris/59/2007 H1 proteins were used as the coating antigen to assess serum IgG titer. Y axis represented serum dilution titer.

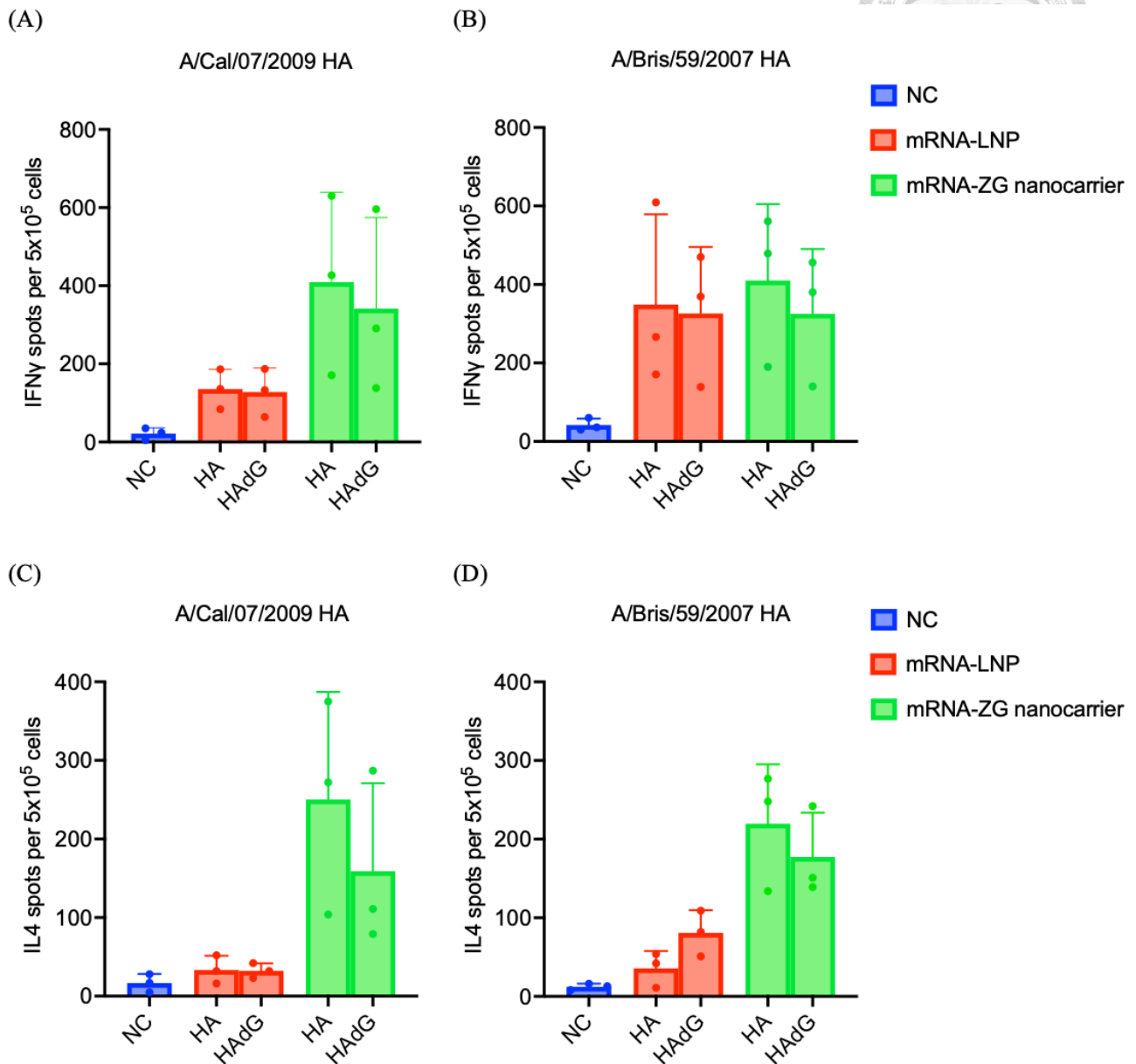
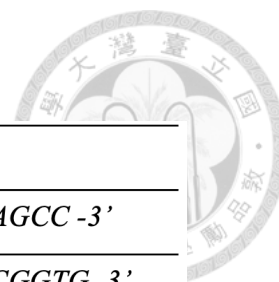


Figure 21. ELISpot analysis of splenocytes from HA and HA Δ G mRNA immunized mice.

(A), (B) IFN γ spots per 5x10⁵ splenocytes were measured by ELISpot with two different strains of H1 protein stimulator, A/Cal/07/2009 and A/Bris/59/2007. Symbols represent individual mice. Heights of bars indicate the mean.



Sites	Primers
<i>N28</i>	5'- CACGGTGTCGGTGCTctgGTTGGCATGGTAGCC -3'
<i>N40</i>	5'- ATGGGTCACGGTCACctgCTTCTCCAGCACGGTG -3'
<i>N104</i>	5'- GGGGTAGCAGGTGCCctgGTCGCTGCTGGGGGT -3'
<i>N304</i>	5'- GAAGGGCAGGCTGGTctgGATGGCGCCCTTGGG -3'
<i>N498</i>	5'- GTAGTCGTAGGTGCCctgCTTCACGCTCTCCATGC -3'
<i>N557</i>	5'- GCACTGCAGGCTGCCctgGCTGCACATCCAGAAGC -3'

Table 1. The primers used for mutation of N-glycosylation sites